CANADIAN THESES

THÈSES CANADIENNES

NOTICE

The quality of this microfiche is heavily dependent upon the quality of the original thesis submitted for microfilming. Every effort has been made to ensure the highest quality of reproduction possible.

If pages are missing, contact the university which granted the degree.

Some pages may have indistinct print especially if the original pages were typed with a poor typewriter ribbon or if the university sent us an inferior photocopy.

Previously copyrighted materials (journal articles, published tests, etc.) are not filmed.

Reproduction in full or in part of this film is governed by the Canadian Copyright Act, R.S.C. 1970, c. C-30.

AVIS

La qualité de cette microfiche dépend grandement de la qualité de la thèse soumise au microfilmage. Nous avons tout fait pour assurer une qualité supérieure de reproduction.

S'il manque des pages, veuillez communiquer avec l'université qui a conféré le grade.

La qualité d'impression de certaines pages peut laisser à désirer, surtout si les pages originales ont été dactylographiées à l'aide d'un ruban usé ou si l'université nous a fait parvenir une photocopie de qualité inférieure.

Les documents qui font déjà l'objet d'un droit d'auteur (articles de revue, examens publiés, etc.) ne sont pas microfilmés.

La reproduction, même partielle, de ce microfilm est soumise à la Loi canadienne sur le droit d'auteur, SRC 1970, c. C-30.

THIS DISSERTATION HAS BEEN MICROFILMED EXACTLY AS RECEIVED

LA THÈSE A ÉTÉ MICROFILMÉE TELLE QUE NOUS L'AVONS REÇUE

NL-339 (r.86/06)

Canada

The Crystal Structures of Some Transition

Metal-Sulphur Complexes

Nasrin Ansari

A Thesis

in

The Department

of·

Chemistry

Presented in Partial Fulfillment of the Requirements

for the degree of Master of Science at

Concordia University

Montreal, Quebec, Canada

August 1983

© Nasrin Ansari, 1983

ABSTRACT

THE CRYSTAL STRUCTURES OF SOME TRANSITION
METAL-SULPHUR COMPLEXES

Nasrin Ansari

This thesis reports the results of the crystal structure determination of three transition metal complexes containing catenated sulphur ligands, using X-ray diffraction techniques. The compounds were prepared in the laboratory of Dr.A.Shaver of McGill University .

The first complex is a Platinum complex, cis-$(PPh_3)_2Pt(C_8H_4NO_2)SSCH(CH_3)_2$ formed by the oxidative addition of the S-N bond of NPhtSSR (where R = $CH(CH_3)_2$, $CH_2CH_2CH_3$, $CH_2C_6H_5$, p-$C_6H_4CH_3$, NPht.) to $(PPh_3)_2Pt(C_2H_4)$. It is the first platinum disulphane complex isolated. The geometry around platinum is found to be square planar, with deviations in bond angles and bond distances similar to other comparable complexes. The important feature of this complex is the torsion angle of 89.5°.in the M-S-S-R linkage.

The second complex is a tungsten complex,

$(\eta^5\text{-}C_5H_5)W(CO)_3\text{-}SS\text{-}\underline{p}\text{-}C_6H_4CH_3$. Tungsten disulphane is stable in the solid state but tends to lose sulphur upon standing in solution. A S-S torsion angle of $63.1°$ is observed.

The third and the last complex is a titanium complex, $(\eta^5C_5H_5)_2Ti(SSSC_6H_5)(SC_6H_5)$. The most interesting feature is the presence of three sulphur atoms in a chain. A structure of this type is previously unreported and is a rare example of metallotrisulphane.

This Thesis

is

Dedicated

to

my Parents

ACKNOWLEDGEMENT

I wish to express my deep appreciation to Dr.P.H.Bird for his continued guidance and encouragement throughout the course of this work and also for providing all the facilities during the preparation of this thesis.

Thanks are also due to Dr.Serpone and Dr.Colebrook for serving on my research committee.

The financial support in the form of a teaching assistanceship from the Department of Chemistry, Concordia University, Montreal, Canada, is highly appreciated.

Finally, I would like to thank my sisters, Mahjabeen and Lalin, for their help and encouragement.

TABLE OF CONTENTS :

LIST OF FIGURES

LIST OF TABLES :

SECTION I

I-1 INTRODUCTION :

This thesis presents the result of the X-ray crystallographic structure determination of the three complexes :

(i) cis-(PPh$_3$)$_2$Pt($C_8H_4NO_2$)SSCH(CH$_3$)$_2$

(ii) (η^5-C$_5$H$_5$)W(CO)$_3$SS-p-C$_6$H$_4$CH$_3$

(iii) (η^5-C$_6$H$_5$)Ti(SC$_6$H$_5$)(SSSC$_6$H$_5$)

The objective of the study of these compounds is to see how the geometry of the sulphur chains -S$_x$- is modified in complexes containing transition metals.

All three complexes were prepared by Dr.A.Shaver et al. at McGill University, Montreal, Canada. The theme of his work is the formation of sulphur-sulphur bonds in transition metal templates.

The theoretical aspects of single crystal X-ray crystallographic determination are summarized in section II of the thesis. The experimental work carried on three complexes is presented in general terms in section III.

While a catenated sulphur ligand is common to all three structures, the coordination spheres of the metals are very different.

Section IV describes the individual experimental details and description of the structures.

1

THEORETICAL SECTION II

II-1 **UNIT** **CELL** : [1-10]

A crystal consists of atoms arranged in a pattern that repeats periodically in three dimensions.

One can divide two dimensional space into parallelograms. In three dimensions, the space is divided into parallelpipeds.
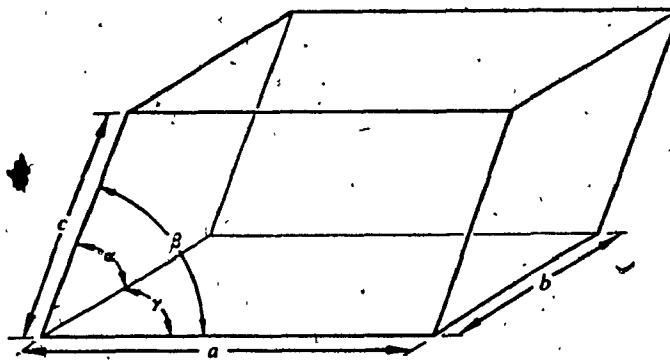
Fig.II-1-1

Repetition of these parallelopipeds by translation from one lattice point to another generates the lattice.

The generating parallelpiped is called a unit cell. A unit cell is the smallest volume of the crystal which contains all the structural and symmetry information for the crystal.

The size and shape of the unit cell may be specified by means of length a, b, and c of the three independent edges and the three angles α, β, and γ between these edges as shown in Fig.II-1-1.

The angle α is the angle between b and c, β is between a and c, and γ is between a and b. These axes define a co-ordinate system appropriate to the crystal.

There are seven crystal systems which give rise to 14 Bravais lattices. The Bravais lattices consist of 7 primitive and 7 non-primitive lattices. The Bravais lattices can be expanded to 32 point groups. Finally 230 space groups have been tabulated which arise from combinations of 32 points groups and 14 Bravais lattices.

II-2 BRAGG'S LAW : [11-14]

The X-ray was discovered by Röntgen (1895), but at that time its nature was not known. It was Max von Laue (1912), who discovered the diffraction of X-rays by crystals. In the same year W.L.Bragg noted the similarity of diffraction to ordinary reflection and deduced a simple equation treating diffraction as reflection.

4

When an electromagnetic wave (having wavelength λ)
strikes two parallel planes, separated by 'd' making an
angle θ , the constructive interference of the waves
generated at points O and C will occur only when θ is
adjusted such that following equation is satisfied. Fig.II-
2-2.

$$n\lambda = 2d\sin\theta \text{ --------------------------------(II-2-1)}$$

This equation is known as Bragg's Law. This
concept can be applied to crystal lattices as they contain
various sets of parallel planes of a stack (hkl) with
spacing d_{hkl}. Fig.II-2-3.

$$n\lambda = 2\ d_{hkl}\ \sin\theta_{hkl} \text{ --------------------(II-2-2)}$$

Fig.II-2-2

5
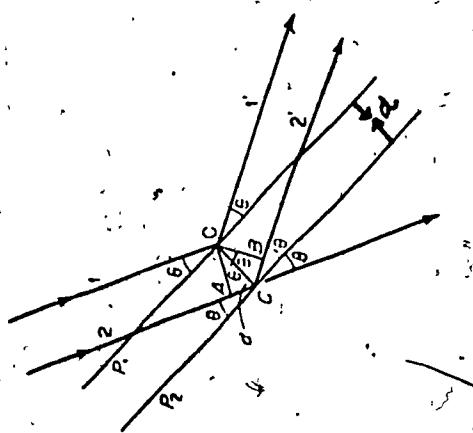
II-3 RECIPROCAL LATTICE : [15-18]

In the unit cell the direct axes are represented as a, b, and c and corresponding interaxial angles as α, β, and γ, Whereas the reciprocal axes are represented as a^*, b^* and c^* and the interaxial angles are α^*, β^* and γ^*. The following picture shows the relationship between the monoclinic direct and reciprocal cell. Fig.II-3-3
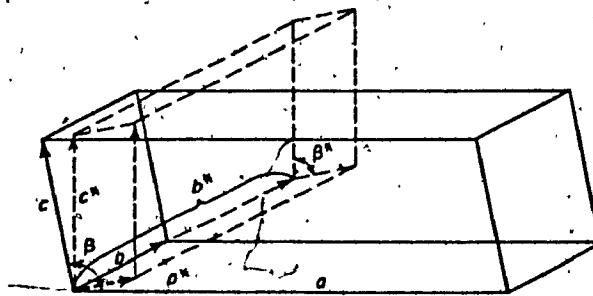
Fig.II-3-3

In order to understand the interpretation of the reciprocal lattice consider a crystal in the X-ray beam having wavelength λ and also consider a*c* section of its reciprocal lattice as shown in Fig.II-3- 4
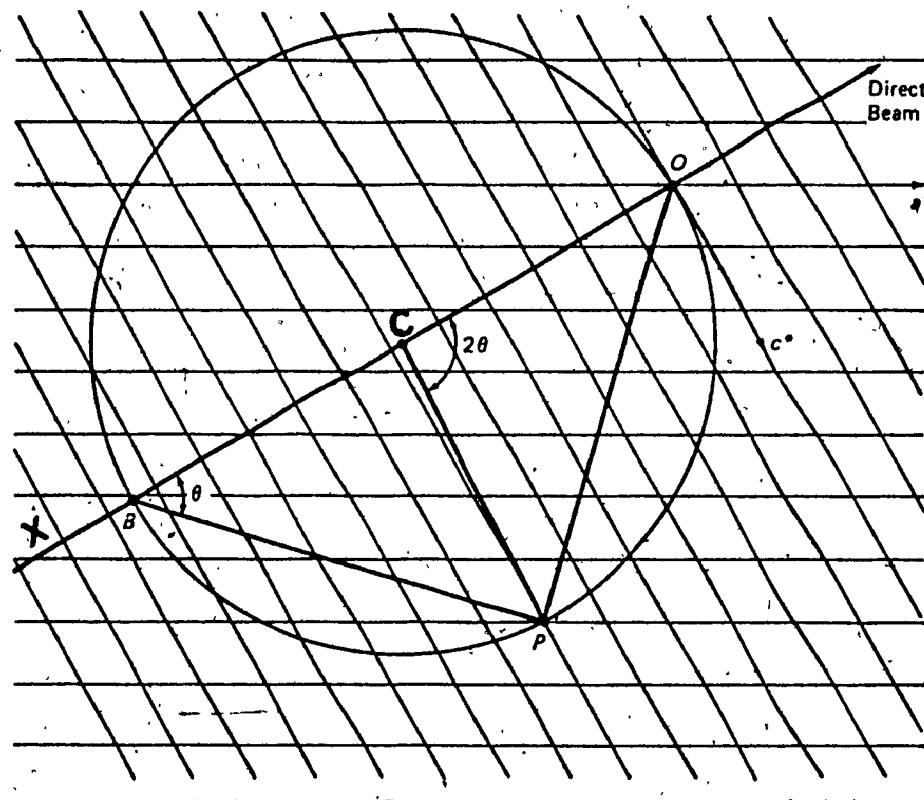
Fig.II-3-4

The crystal is oriented in such a way that the X-ray beam is parallel to the a^*c^* plane. Point O is considered as the origin of the reciprocal lattice and the X-ray beam is allowed to pass in the direction of XO. Construct a sphere of radius $1/\lambda$ centered on line XO, passing through the point O. Keep the sphere fixed and rotate the crystal such that the reciprocal point P falls on the surface of the sphere.

The angle OPB is a right angle and therefore,

$$\sin OPB = \sin \theta = OP/OB = OP/2$$

$$\sin \theta = OP/2 \quad \text{------------------------(II-3-3)}$$

Since P is the reciprocal lattice point the length OP is equal to $1/d_{hkl}$ (this is the way the reciprocal lattice is defined).

Substituting the value of OP.

$$\sin \theta = 1 \ /2 \ d_{hkl}$$

or

$$1 \lambda = 2 \ d_{hkl} \sin \theta \quad \text{---------------------(II-3-4)}$$

Thus whenever a reciprocal lattice point coincides with the sphere constructed as described above, Bragg's law is satisfied and reflection is obtained.

From the Fig.II-3-4 it is evident that the angle PCO is equal to 2θ, so CP makes an angle 2θ with the

8

incident X-ray beam and CP represents the direction of the reflected ray.

The size of the reciprocal lattice constructed in this way depends only on the dimensions of the direct unit cell. When the wavelength of the incident beam is reduced, the sphere of reflection increases in size and vice-versa.

The concept of the reciprocal lattice is quite important in understanding the language of crystallography. Many seemingly involved calculations become quite simple when considered with the help of this concept.

II-4 **ROTATION AND OSCILLATION THEORY** : [19]

Rotation and oscillation photographs are very useful in aligning the crystal on the goniometer head. Also, preliminary information about the crystal symmetry can be obtained from these photographs. The crystal mounted on the goniometer head is placed on the Weissenberg camera and photographs are taken without moving the cassette holding the film. If the crystal is mounted in such a way that it may be rotated about a direct axis, then a reciprocal lattice plane will be perpendicular to the direct axis and therefore perpendicular to the rotation axis. If the crystal is rotated through a small angle, some reciprocal lattice points will cut the sphere of reflection.

Whenever the Bragg condition is satisfied, the diffracted rays will pass from the origin forming cones.
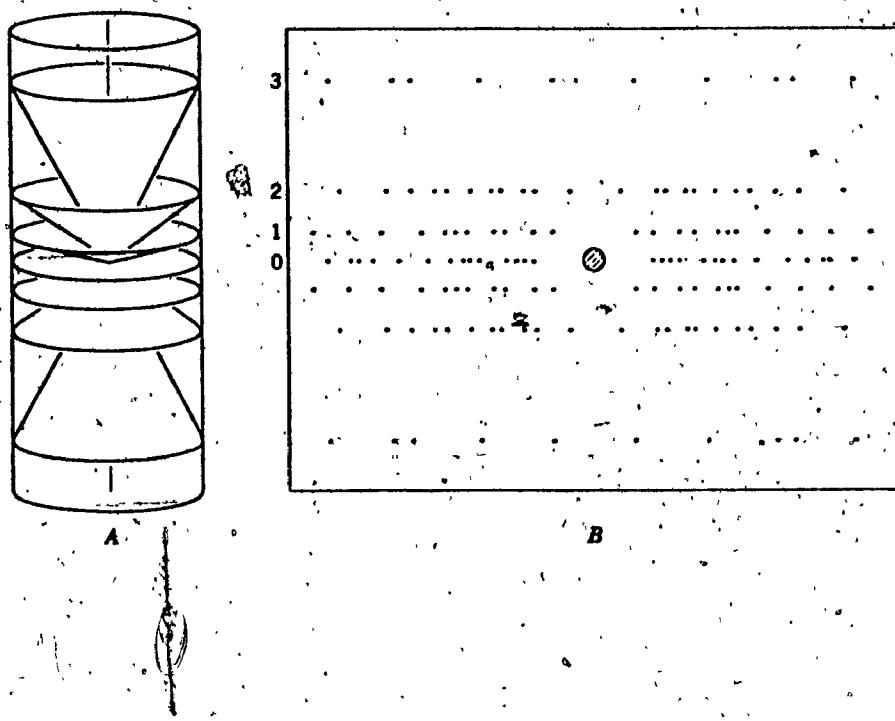
Fig.II-4-5

Each cone represents one reciprocal lattice plane. When these cones fall on the cylindrical film, they are recorded as lines of spots known as layer lines.

From the layer lines it can be deduced whether

the real crystal axis is properly aligned with the rotation
axis. From the spacing between the two layer lines, the
length of the unit cell edge parallel to the axis of
rotation can be calculated.

II-5 **WEISSENBERG THEORY** : [20-21]

In the rotation and oscillation methods, the two
dimensional reciprocal lattice plane is condensed into a one
dimensional layer line.

X-roys
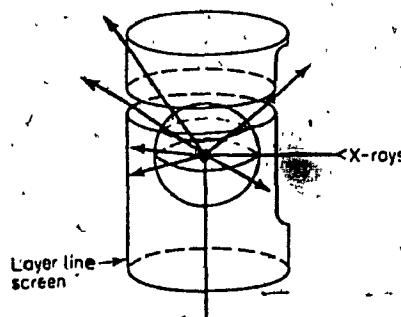
Layer line→
screen

Fig.II-5-6

This disadvantage is overcome in the Weissenberg
technique. A slotted screen, which selects only one layer
line and stops all the other diffracted beams at the same

time is inserted between the crystal and the film. Fig.II-5-6

In order to understand the theoretical interpretation of Weissenberg photographs, consider a reciprocal lattice line which is tangent to the sphere of reflection at the point of exit of the X-ray beam.
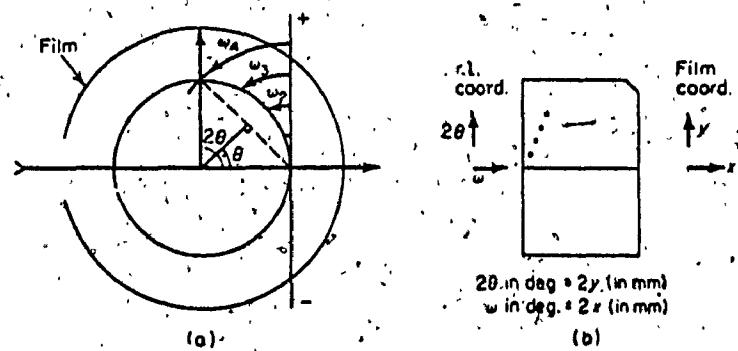
Fig.II-5-7

As the crystal is rotated the central lattice line moves and along with it the reciprocal lattice turns. On the lattice line there are equally spaced lattice points present which give rise to diffractions as they fall on the sphere of reflection, so that the distance of the spot from the central line bears a simple relation to the angle 2θ of the diffracted beam and is proportional to it. The rotation of the crystal and the movement of the camera are coupled in such a way that 2° rotation of the crystal is equal to 1 mm. translation of the film.

(a)   (b)
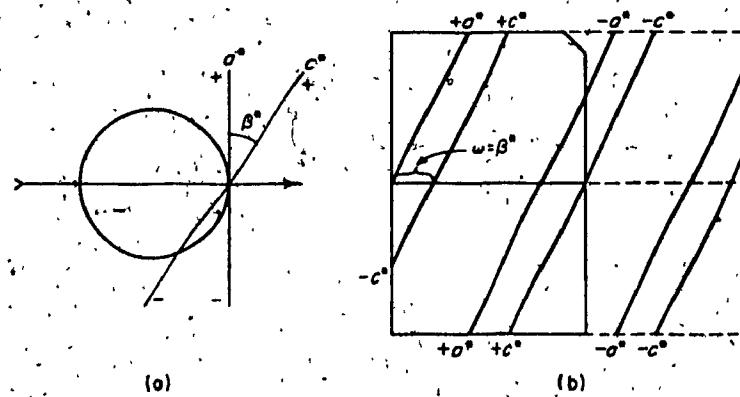
Fig.II-5-8.

The zero level Weissenberg indexing can be explained by considering the reciprocal axis a^* tangent to the sphere of reflection and c^* which makes an angle β^* with it as shown in Fig.II-5-8

13

As the crystal is rotated through 360°, spots generated by a^* will appear on the film. When $\omega = \beta^*$ the c^* will be tangent to the sphere of reflection. Further rotation of the crystal will generate the spots due to the c^* axis in the same fashion as those of a^*. Thus the spots produced by two axis will appear as two straight lines which are off-set from each other by $\omega = \beta^*$ degrees.

II-6 UPPER-LEVEL WEISSENBERG PHOTOGRAPHS :

The equi-inclination technique has the advantage that the upper level photograph is nearly superimposible on the zero level making indexing easier.

The technique requires that the incident beam lies in the cone of diffracted beams for the level being photographed. This is achieved by turning the axis of rotation of the crystal through an angle μ – the equi-inclination angle.
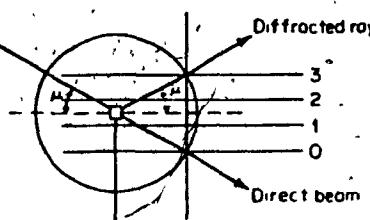
Fig.II-6-9

A set of Weissenberg photographs will give three

dimensional information about the reciprocal lattice which can help to identify the space group and allow the measurement of the cell dimensions. However, reciprocal lattice points lying on or near the rotation axis are not observable. The information can be completed using precession camera techniques.

II-7 PRECESSION THEORY : [22].

Burger (1940) designed the precession camera which gives undistorted photographs of the reciprocal lattice levels. The advantage of the precession photographs as compared to Weissenberg photographs is that the angles and distances of the lattice can be calculated more or less directly from the photographs. Beside this, the lattice plane is easier to index and the symmetry information is more obvious on the photographs.

To understand precession theory, consider a direct axis which is parallel to the incident X-ray beam while the zero level is tangent to the sphere of reflection and at the same time perpendicular to the direct axis and X-ray beam.

Now if the crystal is moved in such a way that it makes an angle with the axis which is perpendicular to the beam, the reciprocal lattice will cut the sphere of reflection on a circle. Fig.II-7-10.

If the crystal is moved such that the direct axis
AO revolves around the X-ray beam and at the same time
keeping angle $\bar{\mu}$ constant, the result will be the
intersection circle revolving about the origin. Any
reciprocal lattice points lying on this circle will give
rise to reflections which are recorded on the film which is
held parallel to the reciprocal lattice level.
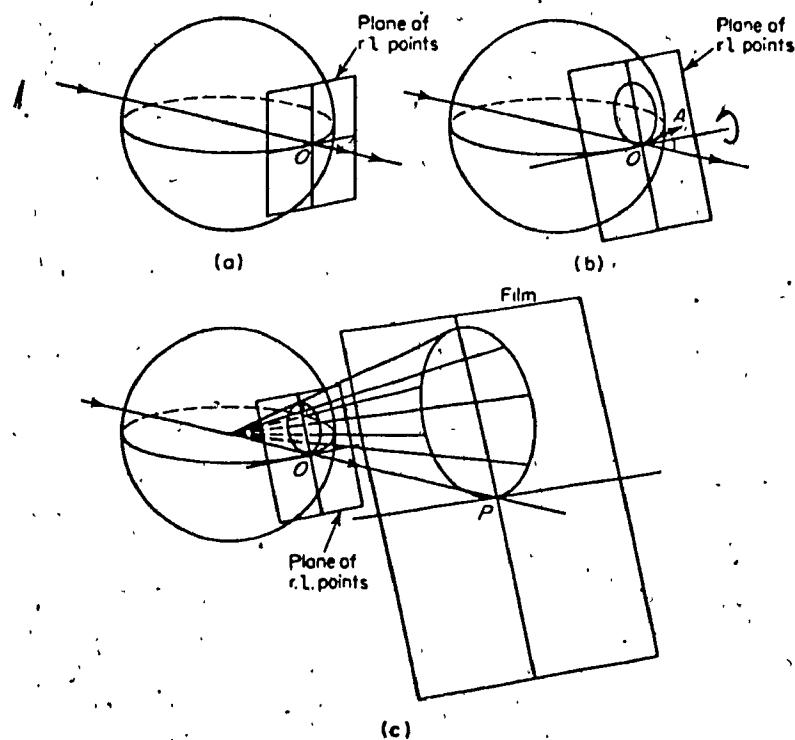
Fig.II-7-10

As the crystal is rotated about the beam the film
precesses about the point P in order to remain parallel to

16

the reciprocal lattice plane. Since P corresponds to the projection of the reciprocal lattice point O, therefore all the other reciprocal lattice points which are projected on the film bear a simple relationship with the point P, resulting in an undistorted picture of the reciprocal lattice.

A suitable screen is used to isolate a particular level net . The screen is a flat metal plate, with a ring cut in it, through which the X-rays can pass. The screen is placed parallel to the film between it and the crystal. The arrangement is such that the cone of diffractions from the plane under consideration will pass through the clear ring to the film. As the crystal moves the screen also precesses, in order to keep the normal through its centre coincident with that through the centre of the cone of reflection.

The Weissenberg camera and Precession camera together provide different information from the same crystal orientation. For example, if a crystal is rotating about the `a' axis a zero level Weissenberg photograph will give `okl' reflections. Without remounting the crystal the Precession camera can give `hol' reflections, when the `b' axis precess about the X-ray beam, and `hko' reflections can be obtained by letting the `c' axis precess.

II-8 **DATA** **COLLECTION** : [23-25]

This section deals with the collection of relative intensities of reflections which are used to deduce the distribution of electron density in the crystal, and from which the arrangement of the molecules in the unit cell can be calculated.

The integrated intensity is a measure of the total number of photons of the characteristic wavelength being used which are diffracted in the proper direction by a reciprocal lattice point passing from the outside to the inside of the sphere of reflection or vice-versa.

A four circle diffractometer is used for the intensity data collecton. It consists of four 'circles' which may be used to adjust the orientation of the crystal so as to bring any desired lattice planes into the reflecting condition.

The two base circles ω and 2θ are mounted on the common axis and either can be adjusted independently or their movement can be coupled. The orienter consists of ϕ and χ circles and is mounted on the ω circle. When $\chi = 0$ the axis of ϕ coincides with ω and 2θ .
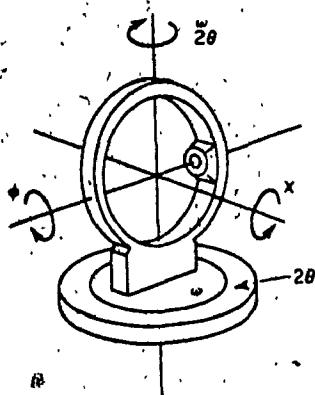
Fig.II-8-11

    While measuring the intensities of the diffraction
spots several problems arise. First of all, the intensities
are usually accompanied by a certain amount of background
radiation which is due to the diffuse scattering of X-rays
of all wavelengths by all the atoms in the crystal and also
by all other objects in the path of the beam. The second
problem is due to the spectral impurities of the incident

beam which leads to white radiation streaks.

A θ-2θ scan technique is generally used to record the integrated intensities of the reflections. The scintillation counter is preferred for MoKα radiation and moves with an angular rate which is twice as that of the crystal.

$$\Delta 2\theta = 2\Delta\omega$$

The counter is linked to a pulse height analyser, which receives pulses from the photomultiplier of the scintillation detector. The pulse height depends upon the energy of the X-ray photons and the number of pulses depends on the number of the X-ray photons.

The value of maximum and minimum 2θ, scan width, scan rate and time for background measurements are specified depending upon the size of the diffraction peak present in the detector. The 2θ angle of the reflection is calculated using an orientation matrix and a reflection is scanned for t_s seconds, as a function of scan width and dispersion factor. The backgrounds are measured at each end of the peak for t_b seconds.

Usually a profile analysis for measuring the reflection is preferred. In this method the reflection profile is examined to determine the point where the background is significantly flat. This point is considered as the point where the peak ends and background begins. The

advantage of using this method is that the quality of the data is improved as compared to usual scan techniques, while using only about half of the time. Also the signal-to-noise ratio is greatly improved.

Sometimes the intensity of the peak is very-high, therefore Ni foil attenuators are used to reduce the intensity of the reflection reaching the counter.

II-9 **DATA REDUCTION** : [26]

The intensity data collected constitute only raw data for structure determination. The following steps are required to produce the `Structure Factors' used in the actual crystal structure analysis.

ELIMINATION OF BACKGROUND RADIATION :

Each peak count is converted into a net intensity by subtracting the background radiation :

$$I = C - (B1 + B2) \, t_s/t_b \qquad \text{------------}(II-9-5)$$

Here, `I' represents the observed intensity, `C' is the peak count, `B1' and `B2' are the high and low background counts respectively, `$t_s$' is the reflection scan time and `t_b' is

the total background time.

The standard deviation $\sigma(I)$ of the intensity I is computed adopting the equation :

$$\sigma(I) = [C + (B1 + B2)/2 \, (t_s/t_b)^2 + (NC)^2]^{1/2} \quad \text{------(II-9-6)}$$

Here, 'N' is the instrumental constant known as 'ignorance factor' and was usually taken as 0.003 during the least square refinement of atomic parameters. Intensities less than a predetermined threshhold $3\sigma(I)$ are rejected along with the reflections which are systematically absent.

SCALING OF INTENSITIES :

The intensities are scaled in accordance with the variation of the three 'standard' reflections repeatedly remeasured during data collection. This corrects for instrument differnce and minor sample decomposition if it occurs.

LORENTZ AND POLARIZATION CORRECTION : [27-28]

The intensity is converted into the structure factor amplitude by the equation:

$$\left| F_{hkl} \right| = \sqrt{K \cdot I_{hkl} / LP} \quad \text{---------------(II-9-7)}$$

Where, 'K' is the scaling factor which depends on the crystal size, beam intensity and a number of other fundamental constants. 'LP' is the Lorentz-Polarization correction. The unpolarized X-ray beam is partially polarized after the reflection from the monochromator and sample crystal and this reduces the measured intensity. The polarization factor corrects the reflection for this effect.

$$p = (\cos^2 2\,\theta_m + \cos^2 2\,\theta_c) / (\cos^2 2\,\theta_m + 1) \quad \text{-----(II-9-8)}$$

'θ_m' and 'θ_c' represent the diffraction angles at the monochromator and crystal respectively.

The time required for a reciprocal lattice point to pass through the sphere of reflection is not constant but varies with its position in the reciprocal space and the direction in which it approaches the sphere. The Lorentz factor corrects for the time it takes for each reciprocal lattice point to pass through the sphere of reflection. For the Picker four circle geometry this factor is :

$$L = 1 / \sin 2\theta \quad \text{--------------------(II-9-9)}$$

These corrections are usually combined as :

$$LP = (\cos^2\theta_m + \cos^2\theta_c)/\sin2\theta_c(\cos^2\theta_m+1) \text{ -------}(II-9-10)$$

II-10 __STRUCTURE FACTOR DEFINITION__ : [29-30]

The structure factor F_{hkl} of a particular reflection expresses the resultant scattering of all the atoms in the unit cell. If N atoms are present in the unit cell, the structure factor for a reflection hkl can be written as

$$F_{hkl} = \sum_{j=1}^{N} f_j e^{2\pi i(hx_j+ly_j+lz_j)} \qquad \text{--------}(II-10-11)$$

Where, (x_j, y_j, l_j) are the fractional co-ordinates of the jth atom and

$$f_j = f_{oj}e^{-B(\sin^2\theta/\lambda^2)} \qquad \text{------------}(II-10-12)$$

The 'f_j' and 'f_{oj}' are the scattering factors of the jth atom in the vibrating and stationary condition respectively.

The structure factor is identified as a complex number, therefore can be analyzed to its real and imaginary parts as:

24

$$F_{hkl} = A_{hkl} + iB_{hkl} \qquad \text{------------(II-10-13)}$$

Where,

$$A_{hkl} = \sum_{i=1}^{N} f_j \cos 2\pi(hx_j + ky_j + lz_j) \text{----(II-10-14)}$$

$$B_{hkl} = \sum_{i=1}^{N} f_j \sin 2\pi(hx_j + ky_j + lz_j)\text{-----(II-10-15)}$$

Further the phase δ and amplitude of the structure factor can be expressed as :

$$\delta = 2\pi(hx_j + ky_j + lz_j) \qquad \text{----------(II-10-16)}$$

and

$$F_{hkl} = \sqrt{A_{hkl}^2 + B_{hkl}^2} \qquad \text{----------(II-10-17)}$$

The phase angle 'α_{hkl}', can be caculated using equation (II-10-18)

$$\alpha_{hkl} = \tan^{-1}(B_{hkl} / A_{hkl}) \qquad \text{--------(II-10-18)}$$

25

II-11 THE RELATIONSHIP OF STRUCTURE FACTORS AND INTENSITIES.: [31-32]

In the X-ray diffraction experiment the most important quantity that is measured is the relative intensity of a reflection hkl. The observed intensity I_o is related to the structure factor by :

$$I_o(hkl) = K^2 C(hkl) \left| F_o(hkl) \right|^2 \qquad \text{-----------(II-11-19)}$$

Here, 'K' is the scale factor associated with $F_o(hkl)$ and 'C(hkl)' depends upon a number of experimental conditions, especially Lorentz and Polarization and sometimes absorption corrections.

The complex quantity, F_{hkl} can be represented on an Argand diagram.
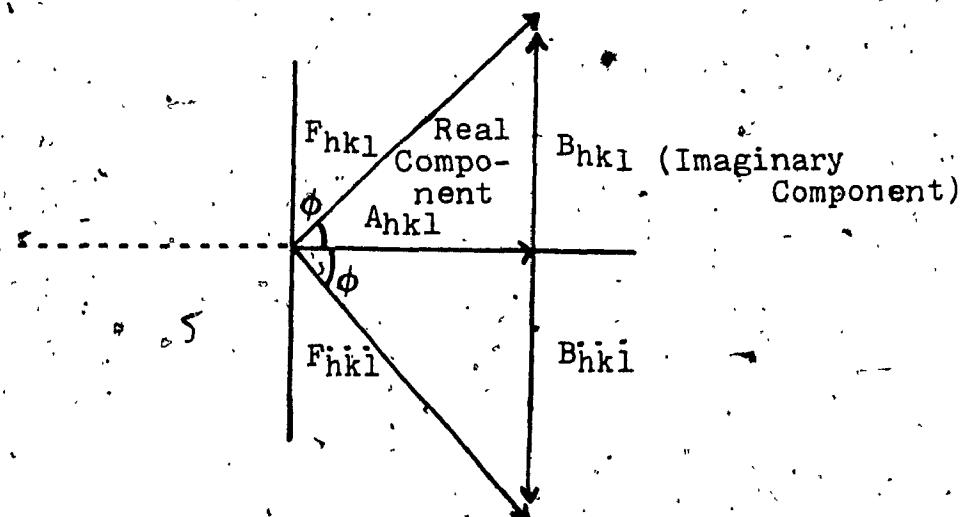
Fig.II-11-12

The complex conjugate of F_{hkl} is $\widetilde{F}_{hkl}$.

$$F_{hkl} = A_{hkl} + iB_{hkl}$$

$$\widetilde{F}_{hkl} = F_{\bar{h}\bar{k}\bar{l}} = A_{hkl} - iB_{hkl}$$

When F_{hkl} and $\widetilde{F}_{hkl}$ are multiplied together :

$$F_{hkl} \cdot \widetilde{F}_{hkl} = (A_{hkl} + iB_{hkl}) \cdot (A_{hkl} - iB_{hkl})$$

$$I_{hkl} = \left| F_{hkl} \right|^2 = A_{hkl}^2 + B_{hkl}^2 \quad --------(II-11-20)$$

It can also be shown that for reflections hkl and its centrosymmetric related partners hkl,

$$F_{(hkl)} = F_{(\bar{h}\bar{k}\bar{l})}$$

which means,

$$I_{o(hkl)} = I_{o(\bar{h}\bar{k}\bar{l})} \quad ----------(II-11-21)$$

This is Freidel's law. The recorded diffraction pattern will appear centrosymmetric, even though the structure itself

27

does not possess a centre of symmetry. Deviation from Freidel's law occurs when an anomalous scatterer is present in the structure.

II-12   COMPARISON OF CENTRO- AND NON-CENTROSYMMETRIC STRUCTURE FACTORS :

A centrosymmetric crystal is considered to possess centre of symmetry at the origin of the unit cell. If an atom is present at x_j, y_j, z_j an identical atom is present at $-x_j, -y_j, -z_j$. The equation (II-10-11) may be written in the form,

$$F_{(hkl)} = \sum_j f_j \left[\cos2\pi(hx_j+ky_j+lz_j)+\cos2\pi(-hx_j-ky_j-lz_j)\right]$$

$$+i \sum_j f_j[\sin2\pi(hx_j+ky_j+lz_j)+\sin2\pi(-hx_j-ky_j-lz_j) \quad ---(II-12-22)$$

or

$$F_{hkl} = 2 \sum f_j\cos2\pi(hx_j+ky_j+lz_j)$$

or

$$A_{hkl} = 2 \sum f_j\cos2\pi(hx_j+ky_j+lz_j)$$

28

i.e.

$$F_{hkl} = A_{hkl} + i0 \qquad (B_{hkl}=0) \qquad \text{---------------(II-12-23)}$$

The phase angle 'α_{hkl}' is restricted to either 0° or 180° for centrosymmetric structures and structure factor can be determined by either a '+' or '-' sign. However, in some noncentrosymmetric structures F_{hkl} the phase may have a special value depending upon the space group symmetry.

In the case of noncentrosymmetric structures the phase angle can have any value from 0 to 2π.

II-13 FOURIER SYNTHESIS : [33]

Since crystals are periodic in structure, the electron density can be described as a periodic function by means of a Fourier series which is the sum of sine and cosine terms with appropriate co-effcients. The electron density thus calculated is the Fourier transform of the structure factors and related to F_{hkl} by equation :

$$\rho(x,y,z) = 1/V \sum_{h} \sum_{k} \sum_{l} \left| F_{hkl} \right| \cos 2\pi(hx+ky+lz-\alpha'_{hkl}) \quad \text{-----} \text{(II-}$$

13-24)

An electron density distribution calculated by a Fourier synthesis using the observed structure factors is called an " Observed Fourier " map.

A " Difference Fourier " is frequently used when a structure is partially solved, to search for comparatively light atoms e.g. hydrogen. The co-efficient ΔF can be used in the difference Fourier summation.

$$\Delta \rho_{(x,y,z)} = 1/V \sum_h \sum_k \sum_l \Delta F \cos 2\pi(hx+ky+lz-\alpha'_{hkl}) \quad \text{----(II-13-24)}$$

where;

$$\Delta F = \left| F_o \right| - \left| F_c \right|$$

and

$$\cos \alpha = A / \left| F_c \right|$$

$$\sin \alpha = B / \left| F_c \right|$$

Here, F_o is the observed structure factor, F_c is the structure factor calculated using equation II-10-11. "A" and "B" are the cosine and sine terms in the structure factor calculation. For a centrosymmetric case the sine term is

30

zero. The usefulness of a D-Fourier arises because it removes the contribution to $\rho_{(x,y,z)}$ of all atoms included in structure factor calculation at that stage.

II-14 **THE PHASE PROBLEM** : [34]

The stucture factor $F_{(hkl)}$ is related to the intensity as has already been described in sect.(II-11). Unfortunately, the structure factor is not just a positive number but a complex conjugate having both magnitude and phase. The magnitude can be calculated by measuring the intensities of reflections, but there is no way to measure the phase of the structure factor; hence the "Phase Problem". There are two basic ways to overcome this problem.

(i) the heavy atom method.

(ii) direct method.

THE HEAVY ATOM METHOD : [35-38]

It is possible to locate the heavy atom in the crystal cell by this method. Once the heavy atom in the cell is located it can serve as a phasing model from which the other atomic positions can be developed. A Patterson synthesis provides a vector map of the contents of the unit cell and is expressed as :

$$P_{(u,v,w)} = 1/V \sum_h \sum_k \sum_l \left| F_{hkl} \right|^2 \cos 2\pi(hu+kv+lw) \quad \text{----(II-14-25)}$$

Thus a peak at the point uvw in a Patterson map indicates that atoms are present at x_1, y_1, z_1 and x_2, y_2, z_2 in the crystal such that :

$$U = x_1 - x_2$$

$$V = y_1 - y_2$$

$$Z = z_1 - z_2$$

A unit cell containing N atoms will have $N^2 - N/2$ independent patterson peaks, excluding the intense peak at the origin. Since the cell of the Patterson synthesis is of the same size as that of the crystal, the peaks are obviously much more densely packed and they overlap each other. This can be minimized by using " Sharpened Structure Factors " (where atoms are considered as point scatterers

$$(F_{sharp})^2_{hkl} = \frac{[0.1667+(\sin^2\theta)/\lambda^2]\,[F_{obs}]^2 hkl}{[\sum fo_j e^{-B(\sin^2\theta/\lambda^2)}]} \quad \text{-----(II-14-26)}$$

32

The term `B' is the average thermal parameter, and `fo$_j$' is the mean atomic scattering factor of the jth atom. The weight of the Patterson peak depends upon the product of the atomic numbers of atoms defining the vectors. The major significance of this peak height relationship is that the vectors between like heavy atoms appear with weights corresponding to the square of their atomic numbers, and they may be very prominent against the background of heavy-light and light-light atom vectors. If the asymmetric unit contains few heavy atoms, their location is straight forward. However, if the structure is more complex then with or without heavy atoms it will be more difficult to assign peaks to specific vectors.

DIRECT METHODS : [39-44]

In the early days of its development, direct methods were limited almost entirely to the centrosymmetric space groups. Phasing consisted of assigning a plus or minus sign to each observed structure amplitude. However, the phase solution of non-centrosymmetric crystals by direct methods is now becoming quite common. Sayre(1952) described a method which prov the basis for the routine application of direct methods for the case of centrosymmetric crystals.

$$S(F_{hkl}) \sim S(F_{h'k'l'}).S(F_{h-h',\ k-k',\ l-l'}) \qquad --(II-14-27)$$

or

$$S(F_{hkl}).S(F_{h'k'l'}).S(F_{h-h',k-k',l-l'}) \sim +1 \ ---(II-14-28)$$

Where, `S' means sign and `$\sim$' means probably equal to.

The same result is also obtained from the equation of Hauptman and Karle(1953)

$$S(E_A) = S(\sum_{A=B+C} E_B.E_C) \qquad ---------(II-14-29)$$

Here, `S' means `sign of' ; A,B,C are the vectors (hkl) for reflections A,B,C ; E_A, E_B, E_C are the normalized structure factor for reflections A,B,C. The normalized structure factor is defined as :

$$E_h = F_h \ / \ \epsilon \ [\sum \ f_{jh}^2]^{1/2} \qquad --------(II-14-30)$$

F_h' is the structure factor for reflection h; N is the total number of atoms in the unit cell. `f_{jh}' represents the atomic scattering factor for the jth atom for the value of associated with h and ϵ is a "statistical fudge factor" adjusting for the degeneracy in F for reflections at symmetry locations in reciprocal space. A typical procedure, the one used in Multan , is as follows :

A list of both observed and calculated values of E vs 2θ is obtained. The E's are scaled in such a way that the mean $E^2 = 1$. All the strong reflections are chosen which have the value of E greater than a specified value. In addition some of the weakest reflections are also found. All strong triples h,k,l; h'k'l'; h-h',k-k',l-l' (called $\sum^2$ relationships) are sorted out within this set, plus those for the weak hkl's where the other two reflections are strong. This weak group is known as the ϕ zero reflections.

All strong reflections among the $\sum^2$ reflections are tested by using the quantity $\langle \alpha^2 h \rangle$. If the reflections are useful they are used early in the phase solution.

$$\langle \alpha^2 h \rangle = \sum_{h'} K_{hh'} + \sum_{h'} \sum_{h\,h'} K_{hh'} K_{h'h''}.X \quad \text{---(II-14-31)}$$

where,

$$X = \frac{I_1(K_{hh'})\ I_1(K_{hh''})}{I_0(K_{hh'})\ I_0(K_{hh''})} \quad \text{----(II-14-32)}$$

'I_0' and 'I_1' are Bessel functions and $\langle \alpha^2 h \rangle$ mean the expectation value of $\langle \alpha^2 h \rangle$

The exact probability that eq.(II-14-27) is

correct is quite important. The probability is expressed as :

$$P = 0.5 + 0.5 \tanh \left\{ (\sigma_3 / \sigma_2^3) \left| U_{hkl} \cdot U_{h'k'l'} \cdot U_{h-h', k-k', l-l'} \right| \right\}$$

$$----------(II-14-33)$$

'P' is the probability that eq.(II-14-33) will hold.

$$\sigma_3 = \sum_{i}^{N} n_i^3$$

$$\sigma_2 = \sum_{i}^{N} n_i^2$$

and

$$n_i = f_i / \sum_{i} f_j \qquad ------(II-14-34)$$

where 'f_i' and 'f_j' are the scattering power of the ith and j^{th} atom respectively.

II-15 ORIGIN DEFINITION : [45]

The application of direct methods requires a set of reflections with known phases to start from. A set of upto three known phases can be obtained by the definition of the origin.

The origin always coincides with an inversion
centre in the case of the centrosymmetric crystal. In every
centric unit cell eight inversion centres are present. The
possible positions are (0,0,0), (1/2,0,0), (0,0,1/2),
(1/2,1/2,0), (1/2,0,1/2), (0,1/2,1/2) and (1/2,1/2,1/2).
These eight centres are not identical, therefore for the
origin definition purposes the reflections are categorized
in eight parity groups, eee, oee, eoe, eeo, ooe, oeo, eoo
and ooo, where 'o' stands for odd and 'e' stands for even.

Fig.II-15-13

37
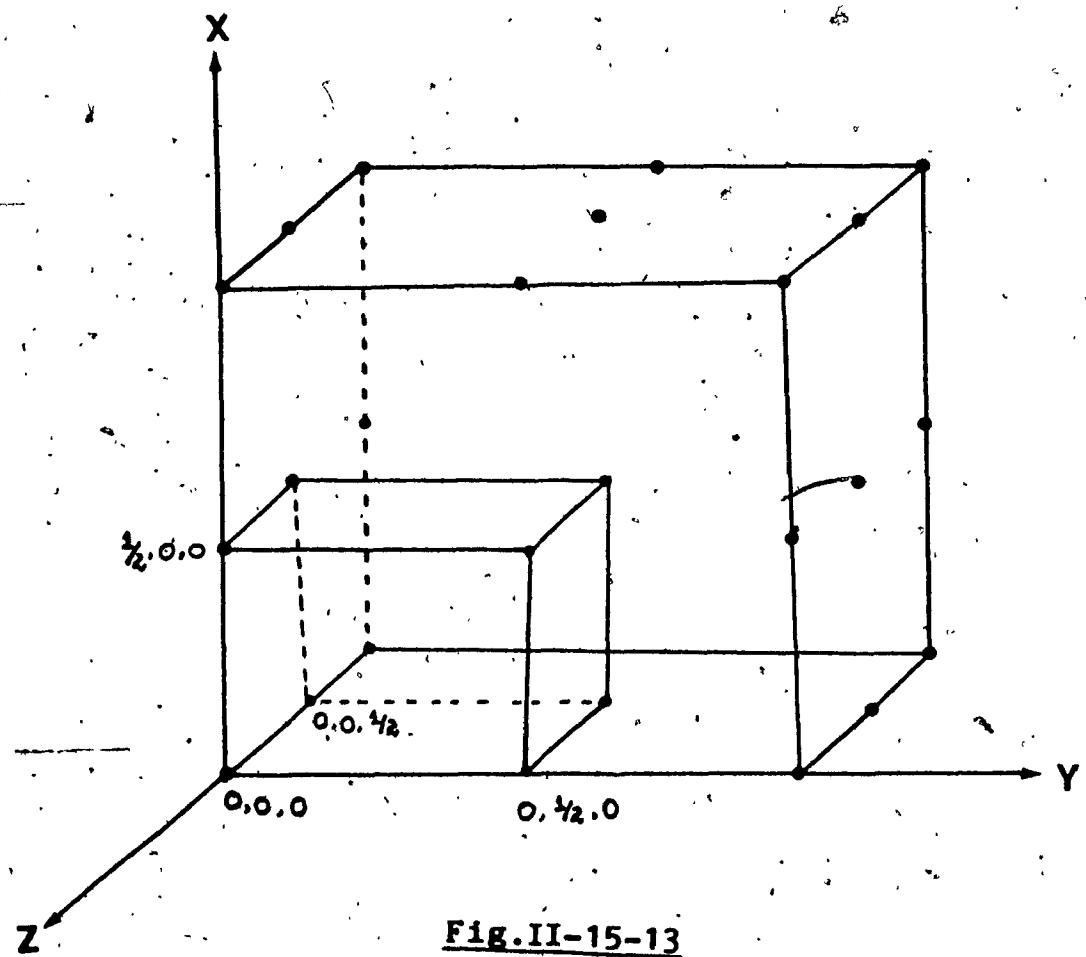
A set of three reflections are chosen in such a way that any reflection indices or any vector sum of two does not give an eee combination. Arbitrary phases are assigned to these reflections. The effect is to select a particular inversion centre type as origin.

A similar selection is made among other type of symmetry elements in the case of the non-centrosymmetric structure.

II-16 LSTSQ REFINEMENT THEORY : [46-50]

The structure factor for a particular reflection(hkl) is calculated using

$$F_c = \sum f^c_{o_j} e^{-2B_j(\sin^2\theta/\lambda^2)} e^{2\pi i(hx_j+ky_j+lz_j)} \quad --(II-16-35)$$

where

F_c = calculated structure factor

$f^c_{o_j}$ = free atom scattering factor of the jth atom

x,y,z = positional co-ordinates

B_j = isotropic thermal parameter

$B = 8\pi\mu^2$

38

For anisotropic vibration, 'B' is replaced by six parameters and is given by the equation :

$$f = f_{0j}e^{-(\beta_{11}h + \beta_{22}k + \beta_{33}l + 2\beta_{12}hk + 2\beta_{13}hl + 2\beta_{23}kl)} \quad \text{--(II-16-36)}$$

The equation approximates the amplitude and direction of vibration as an ellipsoid. An equivalent and preferable expression for the temperature factor is :

$$[-2\pi^2 U_{11}h^2a^* + U_{22}k^2b^* + U_{33}l^2c^* + U_{12}hka^*b^* + U_{13}hla^*c^* + U_{23}klb^*c^*]$$

$$\text{-----------(II-16-37)}$$

Here, 'U' represents the thermal parameter expressed in terms of mean square amplitude of vibration in Å .

Free electron scattering factors are corrected for relativistic effects before using in the structure factor calculations. Due to the very fast movement of the core electrons , the scattered X-ray photons are out of phase with the incident photons. Thus scattering is considered as inelastic to a significant degree. These corrections are significant in the case of 'heavy atoms' and take the form of a real ' Δf' and imaginary ' Δf" known as dispersion correction.

$$f^{c} \delta_j = f_{oj} + f_{oj+1} \quad f_{oj} \quad \text{-----(II-16-38)}$$

Each atom possesses a positional and thermal parameters as expressed by the eq.(II-16-35). The parameters are optimized by minimizing the difference D between the observed $|F_{obs}|$ and calculated $|F_c|$ structure factors.

$$D = \quad W_{hkl}(\,|\,F_o\,| - |\,kF_c\,|\,)^2 \quad \text{------(II-16-39)}$$

Where

k = scale factor for F_c

and

$$W_{hkl} = 1 / \sigma^2(F_{hkl}) \quad \text{----(II-16-40)}$$

The differential of the equation (II-16-38) with respect to each of the parameters is set to zero. The equation obtained is non-linear and use of truncated Taylor series is required. Thus 'n' linear equations in parameter shifts, ΔP_n are obtained and can be expressed in the form of matrix.

$$\begin{pmatrix} a_{11}a_{12} \text{ -------- } a_{1n} \\ a_{21} \\ \\ a_{n1} \text{ ------------- } a_{nn} \end{pmatrix} \begin{pmatrix} P_1 \\ P_2 \\ \\ P_n \end{pmatrix} = \begin{pmatrix} V_1 \\ V_2 \\ \\ V_n \end{pmatrix}$$

where

$$a_{ij} = \sum_r w_r \, \partial \left| kF_{cr} \right| / \partial P_1 \cdot \partial \left| kF_{cr} \right| / \partial P_j \quad \text{-----(II-16-41)}$$

and

$$v_{ij} = \sum_r w_r \cdot F_r \, \partial \left| KF_{cr} \right| / \partial P_j \quad \text{-------(II-16-42)}$$

This set of normal equations can be written in a more compact form as :

$$AX = V \qquad \text{--------------(II-16-43)}$$

If

$$A^{-1} \cdot A = I \qquad \text{-------------(II-16-44)}$$

then

$$A^{-1} \cdot AX = A^{-1}V$$

or

$$X = A^{-1}V \qquad \text{-----------(II-16-45)}$$

The standard deviation of any parameter is given as :

$$\sigma P_i = \sqrt{b_{ii} \cdot \left(\sum w_{hkl} \Delta F_{hkl}^2\right) / (m-n)} \qquad \text{-------(II-16-46)}$$

Where, b_{ii} represents the ith diagonal of the inverse matrix, w_{hkl} is the weight of the reflection hkl, m is the number of observations and n the number of parameters and $F = (|F_{o\,hkl}| - |F_{chkI}|)$.

In the case where a large number of parameters are refined, the use of a block diagonal matrix is necessary, because of computer storage limitations

In anisotropic case nine parameters are invoved per atom : six thermal parameters and three positional parameters.

The block diagonal matrix constitutes a series of triangular blocks of dimensions 9x9 for each atom as shown in Fig.II-16-14

42
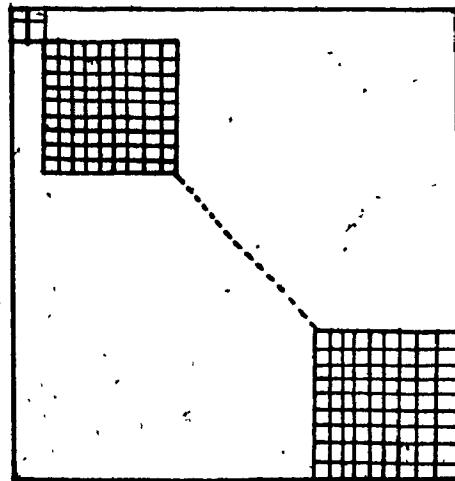
Fig.II-16-14

All interatomic terms of the full matrix are considerd as zero. More cycles are required for the block diagonal Least- Square method than with full matrix to reach convergence.

The correctness and degree of refinement of the structure are related to the residual factor 'R' also known as the "discrepancy factor".

$$R = \sum \left| F_{obs} \right| - \left| F_{cal} \right| / \sum \left| F_{obs} \right| \qquad \text{-----(II-16-47)}$$

or

$$R_w = \sum w \left| F_{obs} \right| - \left| F_{cal} \right| / \sum \left| F_{obs} \right| \qquad \text{----(II-16-48)}$$

43

where

R_W = weighted R factor

The lowest value of `R' and `R_W' correspond to the best fit.

Usually, refinement is stopped when the parameter shifts are less than some fraction (e.g.1/10) of the standard deviation of the parameters.

EXPERIMENTAL SECTION III

III-1 <u>PHOTOGRAPHIC CRYSTAL ALIGNMENT AND CENTERING</u> <u>(WEISSENBERG)</u> :

A fine focus Mo target was used as X-ray source, powered by a Picker Nuclear Generator and Control, Model No.809B, operated at 40KV and 20mA. All the measurements of angles and distances on photographs were carried out using a Charles Supper Co. film measuring device . (Depicted below)
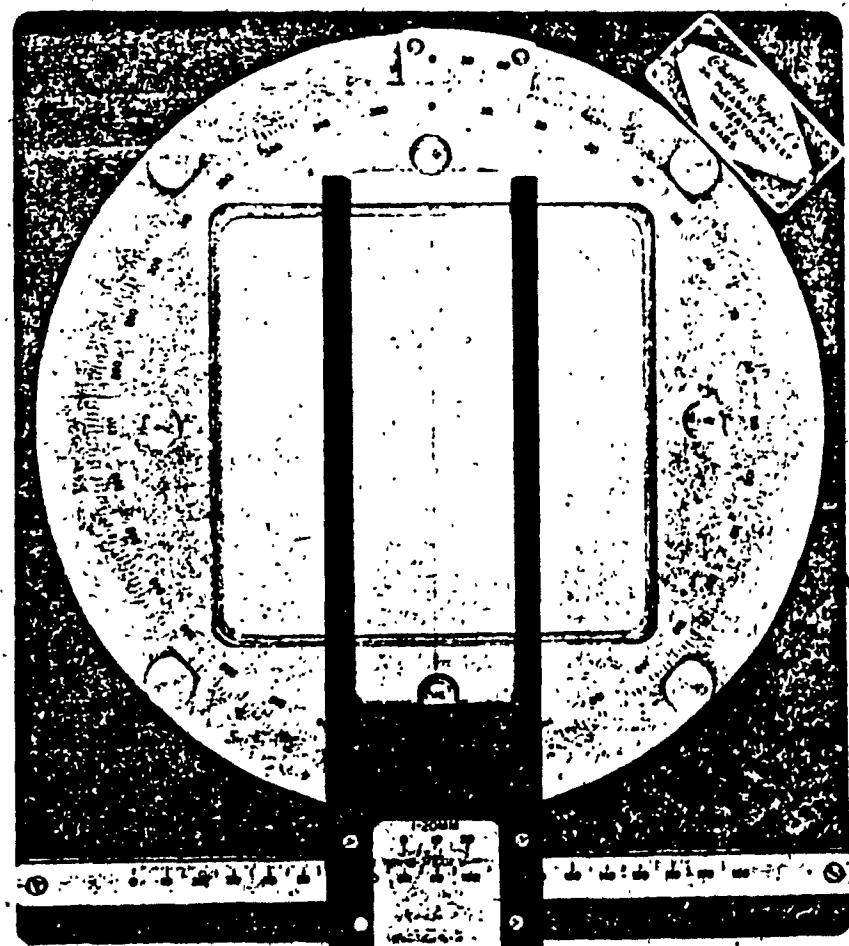
<u>Fig.III-1-1</u>

This device consists of glass plate set in graduated circle which may be rotated in the fixed base and a hair line which slides on a track in the base. Suitable single crystals were mounted on the goniometer head under a Bauch and Lomb stereo-zoom microscope. Crystals were placed on the Weissenberg camera (made by Charles Supper Co., Natick, Mass., U.S.A.) for the rotation and oscillation photographs and were centered on the cross wires of the alignment microscope. The orientation of the crystal must be such that two of its reciprocal axes are perpendicular to the rotation axis. Crystals were photographed while undergoing small oscillation ($\sim 10^\circ$) about ϕ equal to 180° and 270° on the X-ray film. The individual oscillation photographs were exposed for 30 min. Angular errors were measured and necessary corrections were made on the goniometer arcs. The camera was prepared for the second alignment photograph with the cylindrical screen in place. This screen selects only one layer line passing through the slit onto the film.

The photographs were checked for further correction. Sometimes the slit required narrowing a little for selecting only one layer line.

III-2 <u>ZERO LEVEL WEISSENBERG PHOTOGRAPHS</u> :

The rotation angle of 190° was set. (from $\phi = 180^{\circ}$ to 350° passing through zero.) The film holder was allowed to move to and fro within the specified angles and the film was exposed for 48 hrs. For all the Weissenberg photographs a Zr filter was used.

<u>Fig.III-2-2</u>

An illustration of the Zero level Weissenberg Photographs.
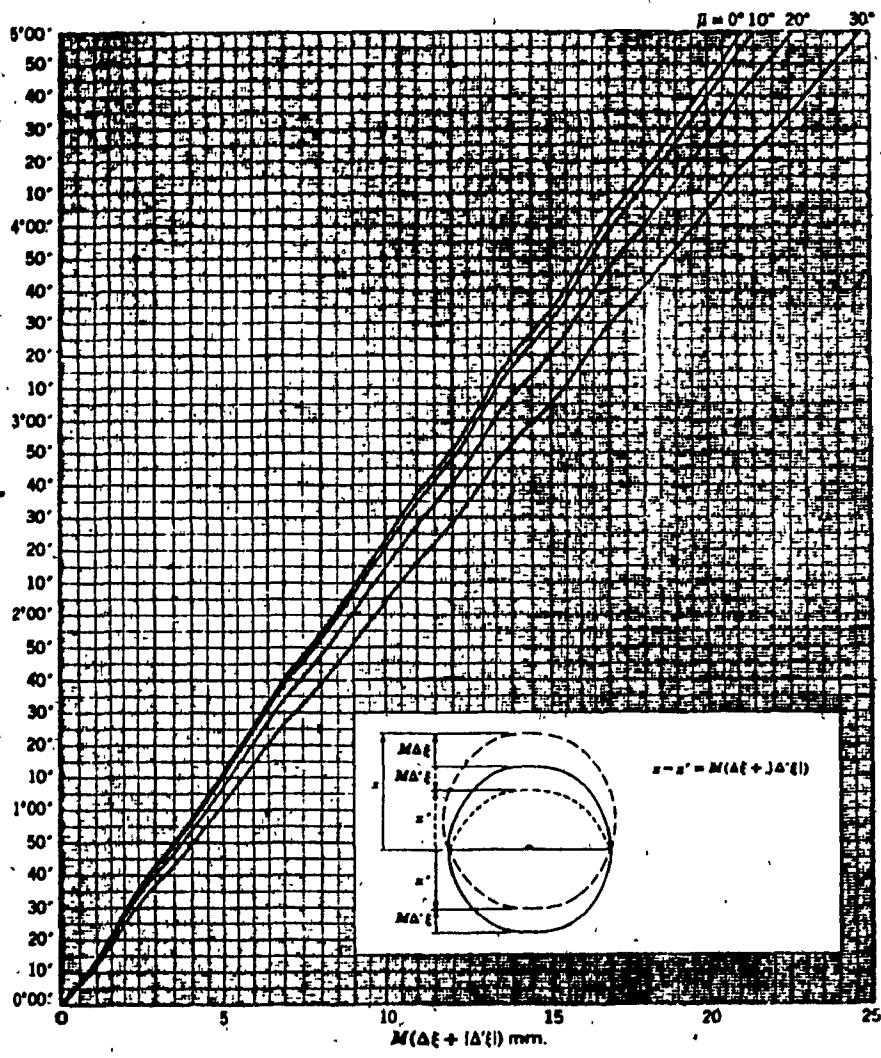
Fig.III-2-3

Chart No.1 : Ref- M.J.Burger " The Precession method in
X-ray Crystallography " N.Y. (1964)

III-3 FIRST LEVEL WEISSENBERG PHOTOGRAPH :

The distance between the zero and the first layer lines on the alignment photograph was measured, which gave the value for the equi-inclination angle and screen setting by consulting the appropriate Chart No.1. After 48hrs. of exposure, the film was developed.
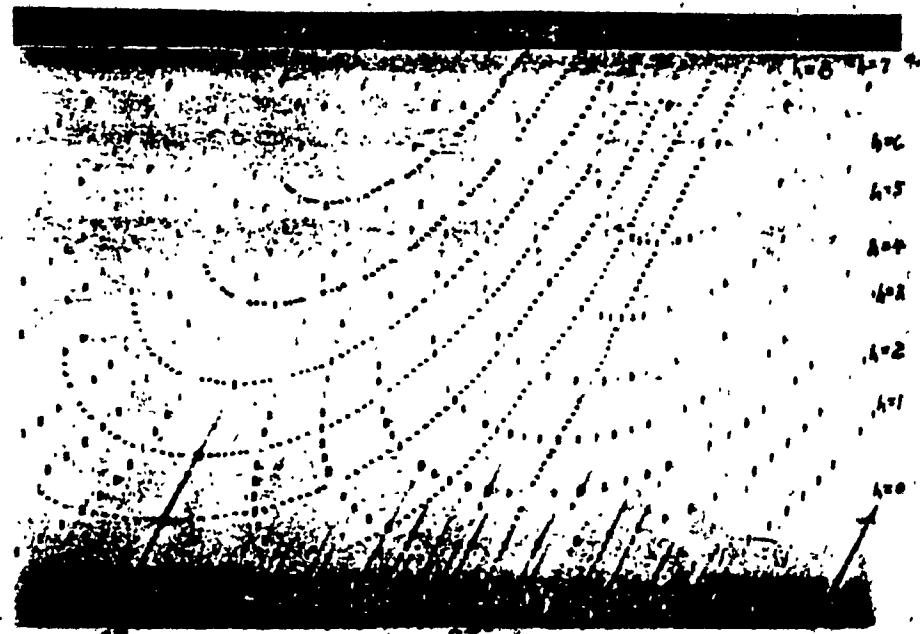
Fig.III-3-4

From the zero level and first level Weissenberg photographs, some information about the space group was available : axis identification and identification of crystal system was usually possible from these photographs.

III-4 ALIGNMENT PHOTOGRAPHS ON THE PRECESSION CAMERA :

The goniometer was transferred to the precession camera. The ϕ value for the axis chosen from the Weissenberg film was set on the precession camera axis. For alignment the crystal was exposed for 20 min. using polaroid film and a precession angle of 10°. No screen or filter were used.
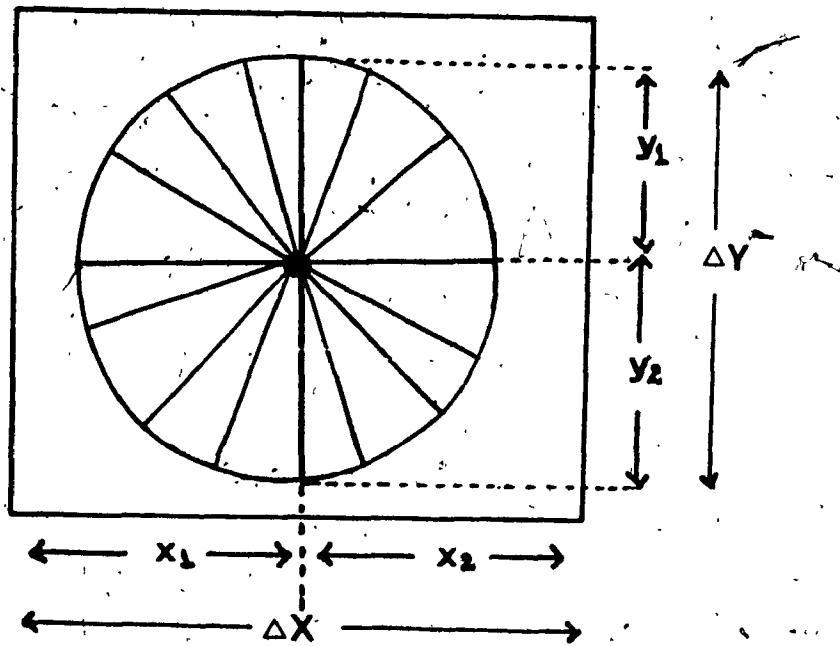
Fig.III-4-5

A diagramatic representation of the alignment photographs on the Precession Camera.

Fig. III-4-5 shows a typical alignment photograph in diagramatic form. The radiating lines are 'white' radiation streaks.

The vertical correction associated with $\triangle y$ is made on the angle ϕ, while the horizontal correction for $\triangle z$ is made to the gonimeter arcs. ($\triangle z$ is resolved into the appropriate components by multiplying by the sine and cosine of ϕ)
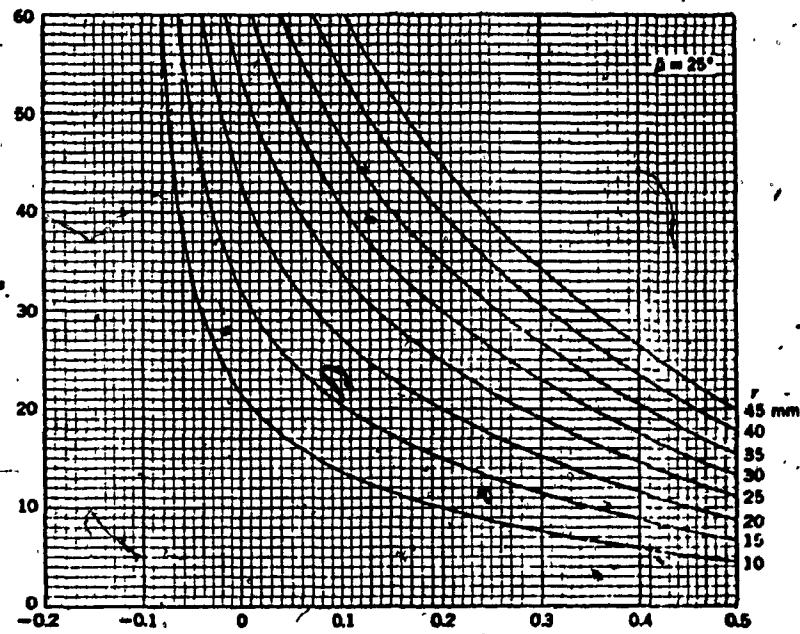
Fig.III-4-6

Chart No.2. : Ref-M.J.Burger " The Precession method in X-ray Crystallography " N.Y. (1964)

III-5 ZERO LEVEL PRECESSION PHOTOGRAPHS :

A precession angle of $25°$ was used and the appropriate Chart No.2, gave the distance of the chosen screen from the crystal. A 48 hrs. exposure using Polaroid film and Zr filter was used.
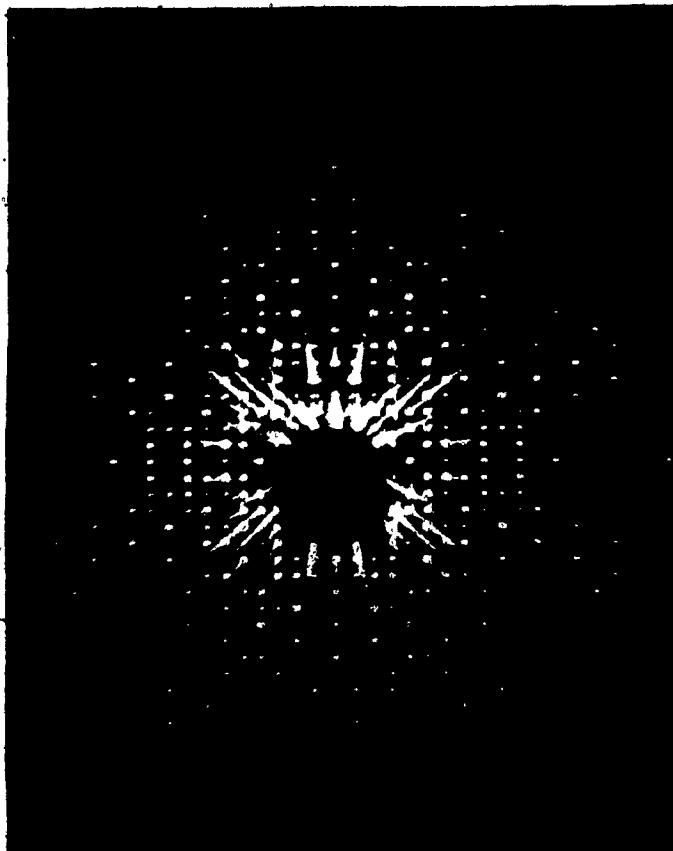
Fig.III-5-7

An illustration of the Zero level Precession Photographs.

III-6 CONE AXIS PHOTOGRAPHS :

The cone axis casette was placed on the screen holder at 32 mm. The photograph was taken with a precession angle of 10° and Zr filter. A 2 hrs. exposure gave the subsequent settings for the upper level photograph. (Depicted below).
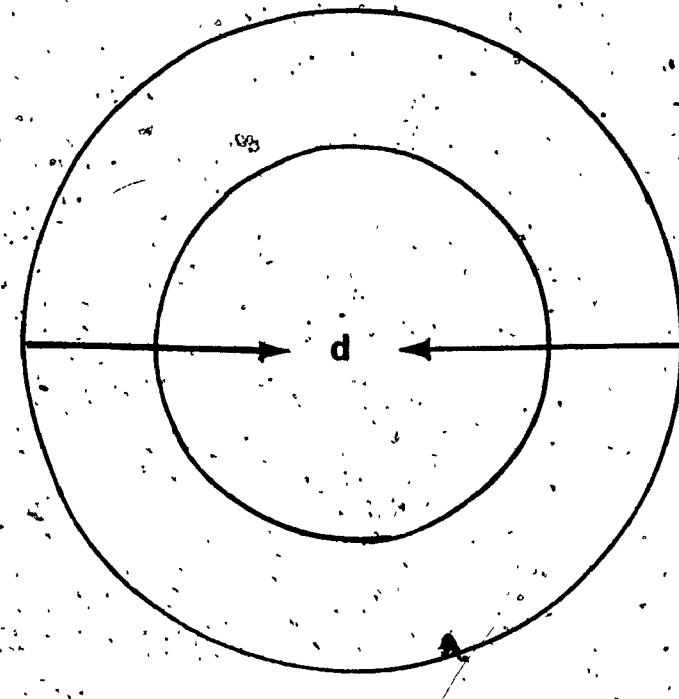
Fig.III-6-8

The diameter of the second ring was measured and a computer generated table was searched for zeta ζ and D settings.

III-7 **FIRST LEVEL PRECESSION** :

A choice of screen size and position that lead to no collision was chosen for a 20° precession angle. (Depicted below).
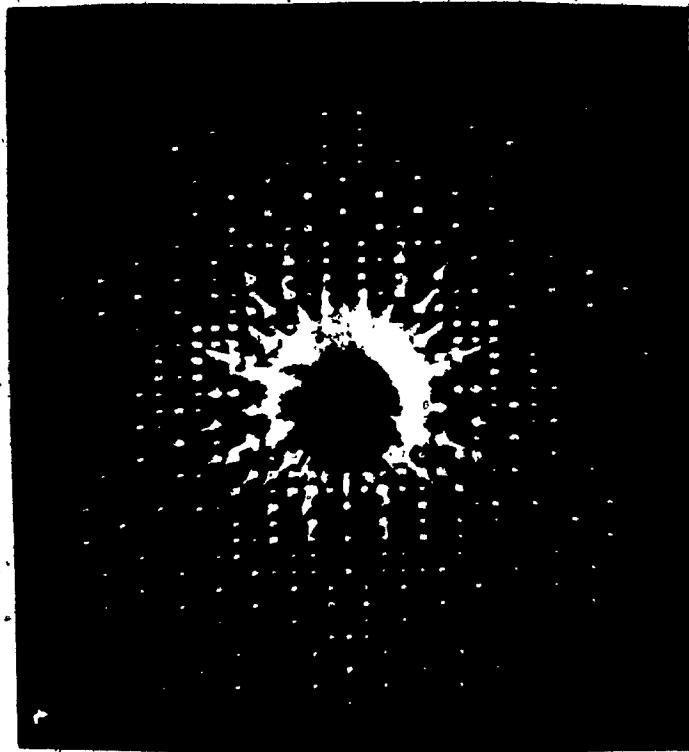
III-8 **SPACE GROUP DETERMINATION** :

The photographic data were used as a guide for determining the space group. In fact only one was encountered : $P2_1/c$.

The two fold screw axis caused the extinction of reflections along an axial line in the reciprocal lattice, (b^* or (ok6) the unique axis, in the case of $P2_1/C$). A c-glide plane affected the reflections in the corresponding

lattice plane, (a^*c^* or hol in the case of P $2_1/C$).

Two Fold Screw Axis   C-glide Plane

Once all the symmetry elements were discovered the determination of the space group was possible. The cell parameters were measured more or less directly from the precession photographs, using the following relationship between the film measured spacing 'x' and reciprocal axis.

$$a^* = x \, / \, 60 \, \lambda \qquad \text{------------(III-8-1)}$$

Where, λ = (0.7107A) is the wavelength of MoKα_1/ Kα_2 radiation filtered with Zr foil. Calculation of b^* and c^*

56

was done in the same way. The volume and later the density
of the crystal were measured :

$$V^* = a^* b^* c^* \sin \beta^* \qquad \text{----------(III-8-2)}$$

or

$$V = 1/V^* = a.b.c \, \sin \beta \qquad \text{----------(III-8-3)}$$

and

$$\text{calculated Density} = n \times M.Wt./ \, V(\text{Å}) \times 10^{-24} \times 6.023 \times 10^{23} \quad \text{------}$$

$$\text{--------(III-8-4)}$$

     If the approximate molecular weight is known then
comparing this value with the total molecular weight of the
cell content, will give the number of molecules per unit
cell. Each space group has a number of asymmetric units
which are to be found in the unit cell and the number
depends upon the symmetry of the space group. If the number
of molecule is less than the number of assymetric units, the
molecule must possess crystallographically imposed symmetry.

III-9 **DATA COLLECTION CONDITIONS** : [51]

The goniometer head, set to Weissenberg settings, was mounted on a Picker Nuclear FACS-1 four circle diffractometer coupled with PDP 8/a computer. A Mo target was used as the X-ray source. The X-ray tube was operated at 40KV and 30mA. The $K\alpha_1$ / $K\alpha_2$ peaks were isolated with a graphite crystal. A 1mm. pinhole collimator was used for the incident beam. The diffracted beam was received in an aperture with vertical and horizontal slits, located 23cm. from the crystal and 20mm. from the scintillation counter. A series of Ni foil attenuators, fixed on a rotating disc were placed automatically between the aperture and the detector to attenuate reflections having intensity greater than 10,000cps. The detector was operated at 1,000 volts and the pulse height analyser was set to recieve 100% of the $K\alpha$ X-ray radiation.

III-10 **CENTERING OF REFLECTIONS** :

During the alignment and data collection the diffractometer control software package by E.Gabe et al. of the NRC Ottawa was used. Some of the commands (keys) that were used are mentioned later in this section.

From the zero level Weissenberg photograph a few reflections were chosen for centering the crystal on the

58

diffractometer. A strong, low angle, axial reflection was chosen; ω, χ, angles were set to zero; and 2θ was adjusted for the chosen reflection. The approximate region of $-\phi$ on the Weissenberg) was searched on the diffractometer. The reflection was centered manually by slowly closing the horizontal and vertical slits and adjusting the angles for maximum intensity, and then the rest of the axis was checked. A high angle reflection was chosen and centered automatically and the angles were recorded. A high angle reflection on the second axis was formed, centered and recorded in the same way.

For centering and alignment of reflections keys `CR' and `AL' were used. `CR' centered the reflections present in the detector by finding the median of the intensity distribution with repect to 2θ, ω and χ. The angles obtained for each reflection (hkl) were saved for subsequent calculations. (M2 and M3).

The two centered reflections and cell parameters were used to locate the third axis using computer routine M2

A third reflection was chosen (from the precession photographs) on or near the third axis. The reflection was found, centered and angles were saved in the same fashion as above.

M3 was used to calculate the orientation matrix and cell from three reflections. Input was hkl, 2θ, ω, χ,

and ϕ for three non-collinear reflections. The real and reciprocal cell parameters were the output.

About 20 reflections of high 2θ value were chosen from the photographs to cover a large volume of the reciprocal lattice and at the same time be fairly intense. These reflections and their corresponding Freidel ($\bar{h}\bar{k}\bar{l}$) equivalents were centered automatically using command `AL'.

The optimized 2θ, ω, χ and ϕ values obtained from these reflections were used for least-squares using `MM'. The variables were the orientation matrix, and the real and reciprocal cell parameters. The cell standard deviations are obtained from the least-square results.

Before selecting appropriate parameters for the scan used in data collection, some idea of the peak width and the accuracy of the orientation matrix was needed, thus, `SR' was used to set angles for a reflection. The line profile of a particular reflection was obtained using `LP': A θ-2θ scan type was chosen to record the integrated intensity of the reflection. The number of points before and after the peaks (25), step size (0.04deg.) and time at each step (0.50sec.) were input. Output was type of scan, starting and finishing values of angles, no. of points, time per point and intensity values. The profile was plotted on the printer. A few reflections were examined in this way.

For the data collection the following information

was required by the computer.

WAVELENGTH AND ORIENTATION MATRIX :

Needed to generate the angles 2θ, ω, χ, ϕ from the indices hkl of a reflection.

MAX. AND MIN. 2θ VALUES AND MAX. HKL :

Needed to restrict the values of hkl generated by the program.

BISECTING MODE AND SCAN PARAMETERS :

Bisecting mode was used in this work : the ϕ circle lying between the tube and the counter, 'ω' was always kept at zero. The remaining settings were such that Bragg's law was satisfied.

The scan was divided into three sections A, B, C, where A and B were fixed and C varied with 2θ such that the value of 2θ was adjusted to cover α_1 and α_2 dispersion. The scan length was calculated by the expression [A+B(tan θ) +C]. Background counts at the ends of the scan were measured for 0.1 of the scan time. The scan speed used was 2.0 deg/min.

61

NO. OF REFERENCE REFLECTIONS AND FREQUENCY :

Three "standards" or "check reflections" were measured every 50 measurement cycles. Their intensities were printed out during data collection.

SPACE GROUP :

Needed so that computer can omit the measurement of reflections satisfying the absence conditions.

DATA COLLECTION :

The data collection was initiated by the command `GO'. The computer offered a strategy for data collection, i.e (how the indices were generated), based on the type of space group.

For P 2_1/c, the only space group encountered in this work, two segments were needed so that no reflection was collected twice, and the data were collected as follows :

Segment 1 : Started at 0,0,0 with l incremented fastest and h slowest

Segment 2 : Started at -1,0,1 with l incremented fastest, k next, and h decremented slowest.

Starting reflections at :	Starting reflections at :
0,0,0	-1,0,1
0,0,1	-1,0,2
0,0,2	-1,0,3
0,0,1	-1,0,1
0,1,0	-1,1,1
0,1,1	-1,1,2
0,1,2	-1,1,3
0,1,1	-1,1,1
0,2,0	-1,2,0
0,2,1	-1,2,1
0,2,2	-1,2,2
0,2,3	-1,2,3
0,2,1	-1,2,1
and so on.	and so on.

Thus on segment 1. all the reflections having indices hkl were collected where as on segment 2 reflections having indices hkl were collected. (Only one quadrant of the reciprocal lattice was required for a unique set of data in $P2_1/c$).

INFORMATION OBTAINED DURING DATA COLLECTION :

The reference reflections were repeated after every 50 reflections. Constancy throughout the data collection indicated that all was well.

A list of all the data which were not saved in the data collection were printed out : these data were rejected due to very weak intensity.

If a reflection was not properly centered in the scan, so that profile analysis failed, a warning message was printed, and the peak count and the two backgrounds were stored in raw form.

III-11 CRYSTAL DATA FILE PREPARATION PROGRAM :

This program initialized a "CD" file which contains all information about the crystal structure such as real and reciprocal cell constants, wavelength used in data collection and number of each type of atom in the cell. In addition space was reserved for atom scattering factor information, absorption data, the scale factor for the data and the atomic co-ordinates and thermal parameters. The atomic scattering and absorption data were used later by the data reduction program. The scale factor was introduced by the normalization stage of data reduction. The atomic co-ordinates and thermal parameters were introduced later by

the editing program and were used during least-square refinements and subsequent calculations.

III-12 **DATA REDUCTION** : [52]

The intensity data obtained up to this stage was the raw data. The previously prepared "CD" file and raw data file (IDATA.DA) were used by the data reduction program (DATDR-2) in the following sequence of steps.

SCALING :

This step scaled the intensities using the reference reflections. Attenuator factors required because attenuators were used during data collection were applied here. The peak count was converted into intensity by using eq.(II-9-5).

GROUPING :

The "GP" file was created. The program reads the data from "I-DATA.DA" (raw data) and groups duplicated or symmetry related observations. This temporary file is used as a directory for the `R' step and was discarded after data reduction.

REDUCTION :

The reflections which were grouped in the 'GP' file were averaged. A reflection was considered insignificant in cases where intensity computed was less, than a multiple of. (I), usually 2 or 3. LP corrections are applied at this step (eq. (II-9-10))

NORMALIZATION :

Before normalizing the structure factors, the values for the effective scattering power of each atom were calculated :

$$f = f_o e^{-B(\sin^2\theta/\lambda^2)} \quad \text{---------------(III-12-5)}$$

Where, 'f_o' is the scattering factor, which is a function of ($\sin^2\theta/\lambda^2$) and 'B' is the thermal parameter, related to mean square amplitude of viberationby the expression :

$$B = 8\pi^2\mu^2 \quad \text{------------------(III-12-6)}$$

An average value of the temperature factor and scale for observed structure factors were computed by the program from a Wilson plot [53] using the equation :

66

$$\ln \bar{I}_{rel} / \sum f_{0i} = \ln C - 2B(\sin^2 \theta / \lambda^2) \qquad ----(\text{III}-12-7)$$

where, $\bar{I}_{rel}$ represents the average observed intensity corrected for Lorentz-Polarization effects taken over a small range of 2θ.

$\ln \bar{I}_{rel} / \sum f_{0i}$ was plotted against 30 ranges of $\sin^2 \theta / \lambda^2$, a straight line fitted to the result. The slope is $-2B$ and intercept is $\ln C$.
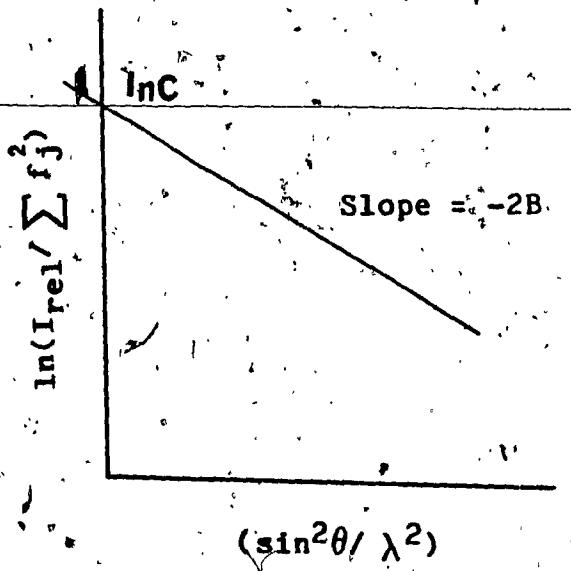
Fig.III-11-10

The term 'C' is related to the scale factor 'K'
thus

$$F_{obs} = 1/\sqrt{C} \ F_{rel} = K \ F_{rel} \qquad \text{------------(III-12-8)}$$

This scale factor was also optimized subsequently in the
least-squares refinement of atomic parameters.

The normalized structure factors which were used
in the statistical phasing process were computed as :

$$E_{hkl} = \frac{\left| F_{hkl} \right|^2}{\epsilon \sum f_i e^{-B(\sin^2\theta/\lambda^2)}} \qquad \text{------(III-12-9)}$$

Here, 'B' represented the average vibrational thermal
parameter obtained from Wilson plot and ' ϵ ' an integer
which usually takes value of 1 but can have other values for
special sets of reflections in certain space groups. For
example, in $P2_1/c$, $\epsilon = 2$ on hol and oko, since for these
sets, half of the spots are missing due to the C-glide
plane and the two fold screw axis, respectively.
Statistically, the other spots present are twice as strong.)

III-13 STRUCTURE SOLUTION :

The structure solution was obtained by either using the heavy atom method or direct methods. The Patterson synthesis was computed using the NRC program FOURR [54] and MULTAN [55] was used in the case of direct method.

III-14 THE HEAVY ATOM METHOD : [56]

For the Patterson synthesis the input required was the CD file and RE file (I_{hkl}'s), output was a list of peaks, from which was deduced the heavy atom position. The heavy atom was used to calculate structure factors using the program LSTSQ [57] and the FOURR was used to calculate an "Observed" or "Difference" electron density map revealing more atom positions. These were added to the 'CD' file using CDEDIT before another structure factor calculation and Fourier, until all atoms were locat

Subsequently, the least-squares refinements were also accomplished using the program LSTSQ . The input for LSTSQ was the CD file and RE file. The output was the CD file with the refined co-ordinates for the atoms along with the refined value of 'K'. Refinements proceeded until the residual indices no longer decreased.

III-15 <u>**DIRECT METHODS : MULTAN**</u>

The first step in this program is the generation of all the triples i.e. h,k,l; h',k',l'; h-h',k-k',l-l'. The next step considers special triples h' = h-h'; k' = k-k'; l' = l-l' known as $\sum 2$ relationships. The phases can be asigned with high probability of correctness for some of the h'k'l'. Thus sign of $E_{2h,2k,2l}$ is probably +ve and independent of the phase of $E_{h,k,l}$ provided both $E_{h,k,l}$ and $E_{2h,2k,2l}$ were strong.

$$S\{E_{2h,2k,2l}\} = S\{E_{h,k,l} - 1\} \qquad \text{------------(III-14-10)}$$

Where, 'S' represented the sign of the E_s taken into consideration.

For the next step, choosing the best starting set, the reflections are ordered according to the strength of their contribution to the phasing process. Repeatedly, the weakest or the poorest is eliminated together with all the triples to which it contributes. Meanwhile, the remaining reflections are tested to check that the origin can still be defined. If not the most recently eliminated reflection is one which defines the origin. The process continues until the necessary number of origin defining reflections is found. These reflections are assigned arbitrary phases. At this stage n (usually 3) more reflections are chosen for inclusion in the starting set. These reflections are

assigned every combination of phases to make 2^n starting sets, each of which is used to phase the rest of the strong data using the tangent formula :

$$\tan \phi_h = \frac{\sum_{h'} w_{h'} \cdot w_{h-h'} \; E_{h'}, E_{h-h'} \; \sin(\phi_{h'} + \phi_{h-h'})}{\sum_{h'} w_{h'} \cdot w_{h-h'} \; E_{h'} \cdot E_{h-h'} \; \cos(\phi_{h'} + \phi_{h-h'})} \qquad\text{(III-14-11)}$$

$\phi_{h'}$ must be 0° or 180° for the centrosymmetric case. When the probability that a predicted phase is correct exceeds a threshhold value (0.98) a new phase is accepted and used to phase more data.

Since 'MULTAN' computes 2^n sets of phases it is necessary to have some figure of merit to indicate the most probable correct phase set. The figures of merit are based on the internal consistency among the reflection phases. (Abs FOM and RESIDUAL) and correct prediction for certain reflections to be very weak (PSI ZERO). A combined FOM is printed which normally allows the choice of the correct phase set.

III-16 **GEOMETRY** : [58]

Bond lengths and bond angles are calculated from the following equations :

$$l = \sqrt{(\Delta xa)^2 + (\Delta yb)^2 + (\Delta zc)^2 + 2ab\,\Delta x\,\Delta y\cos\gamma + 2ac\,\Delta x\,\Delta z\cos\beta + 2bc\,\Delta y\,\Delta z\cos\alpha}$$

-----------(III-15-13)

Where, a, b, c, α, β, γ are the unit cell parameters.

$$\theta = \cos^{-1}\left[(AB)^2 + (AC)^2 - (BC)^2 / 2(AB)(AC)\right]$$ --------(III-15-13)

Where, 'BC' is the non-bonded distance.

Fig.III-16-11

72
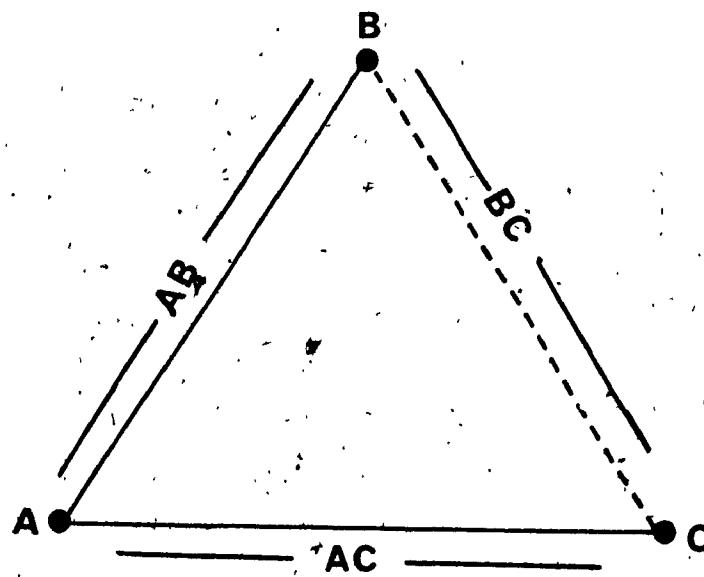
The estimated standard deviation for bond length $\sigma(1)$ and bond angles $\sigma(\theta)$ are calculated according to the following equations :

$$\sigma(1) = \sqrt{(\sigma^2 x_1 + \sigma^2 x_2)(\Delta x/1)^2 + (\sigma^2 y_1 + \sigma^2 y_2)(\Delta y/1)^2 + (\sigma^2 z_1 + \sigma^2 z_2)(\Delta z/1)^2}$$

$$\text{--------(III-15-14)}$$

where, x_1 and x_2 are the estimated average isotropic standard deviations in the x-coordinate of atom1 and atom2 respectively.

$$\sigma\theta = \sqrt{\sigma_2/1_{12} + \sigma^2_1(1_{23})^2/(1_{12})^2(1_{13})^2 + \sigma_3/(1_{13})^2}$$

$$\text{----(III-15-15)}$$

where, ` $\sigma_1$' ` σ_2' and ` σ_3' are standard deviations of atoms 1,2, and 3 respectively. The bond distances and angles were calculated using above equations by the following programs :

DISPOW : [59]

The program calculates the geometry of the molecule from a list of atomic and positional coordinates. The program was sometimes used to deduce a 'molecular structure from a collection of peaks from a Fourier. The output was the final geometry with esd's of bond lengths and angles for the refined structure.

73

UNIMOL : [60]

The program locates a contiguous molecule in cases where the co-ordinates refer to symmetry related pieces of a molecule. The program computes bond distances in a manner very similar to DISPOW, and stores a list of bonds for each atom on the CD file. These lists can be used for calculating hydrogen atom positions.

III-17 **ORTEP** : [61]

The diagrams of the molecular structure represented as "ball and stick" type figures were produced using the program "ORTEP" (Oak Ridge Thermal Ellipsoid Plot Program). Diagrams were drawn on a Nicolet "Zeta" X-Y plotter interfaced with the University CDC Cyber 174. Stereoscopic pairs of figures were also drawn by this program for example unit cell packing diagrams.

CRYSTAL AND MOLECULAR STRUCTURES SECTION IV

IV-1 **INTRODUCTION :**

Organo-sulphur compounds are one of the important features in organic chemistry and bio-chemistry. There are many naturally occuring sulphides and disulphides including penicillins, cephalosporins etc.. Many sulphur cotaining reagents have been developed for S-S bond forming reactions. [62-64].
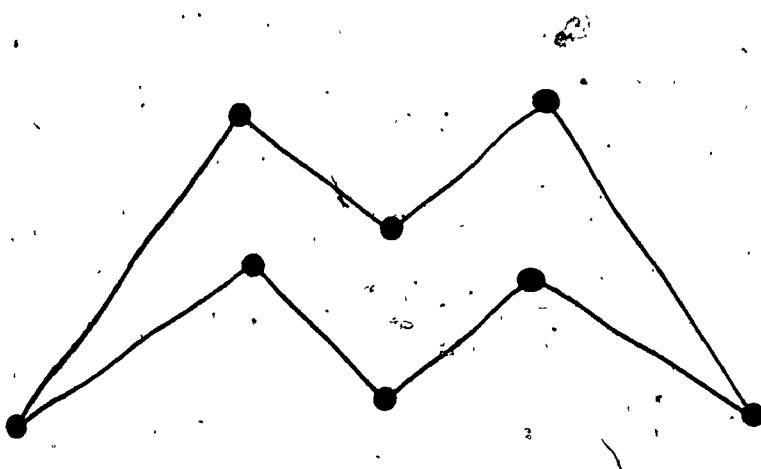
In view of sulphur's pronounced tendency to catenate, it is reasonable to assume the existence of a large class of metal complexes containing simple linear catenated polysulphur ligands. Transition metals and sulphur have great affinity for one another. The main interest in these complexes is due to the fact that they open a wide field in synthetic and theoretical aspects of sulphur chemistry. In addition to this, there is a great interest in sulphur metal interactions because of the catalyst poisoning properties of sulphur compounds.

Sulphur forms a σ-bond using sp^3 hybrid orbitals with metal orbitals of appropriate geometry. However, π-bonding is also possible with an empty 'd' orbital of sulphur and a metal 'd' orbital.
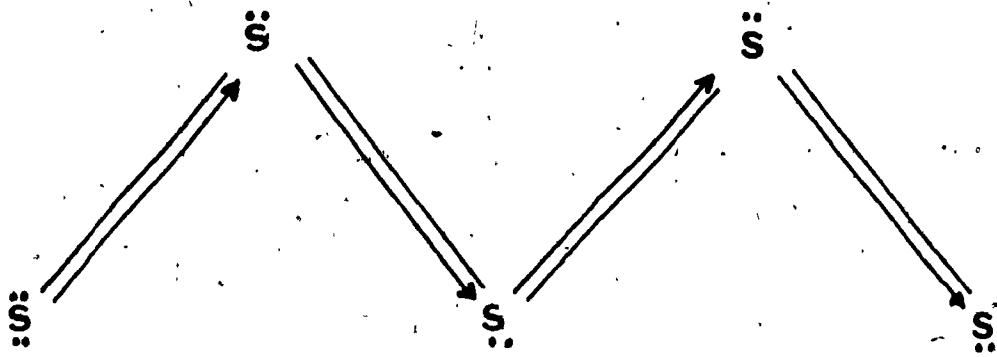
IV-2 **ELEMENTAL** **SULPHUR** :

The first realization of the importance of catenation in sulphur chemistry resulted from early solution molecular weight determinations on elemental sulphur. These studies were conducted in 1900's and suggested that each sulphur molecule was composed of eight sulphur atoms.

S_8 is the most stable form of sulphur. Its crown shaped structure was established from crystal structure studies in 1935 [65] with S-S distance of 2.06Å and dihedral angle of 98°.

Owing to the lone pair of electrons on sulphur atoms, a Zig-Zag chain is formed :
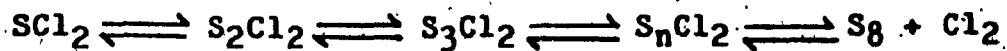
The distance between two sulphurs is 2.06Å and a dihedral angle of 100° is observed. [66].

IV-3 SULPHUR CHAINS :

The Di and "Monochlorides" of sulphur have been known since 1800 as valuable synthetic reagents. [67].

$$SCl_2 \qquad S_2Cl_2$$
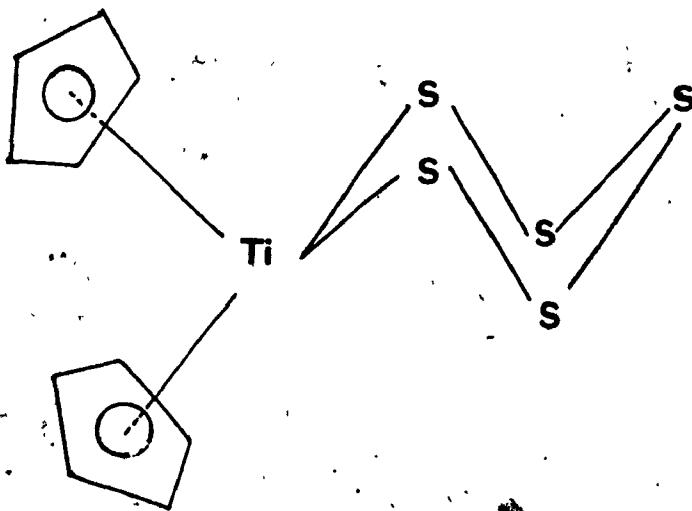
As they possess two leaving groups they can form either polymer chains or rings under appropriate conditions. These reagents are unstable with respect to disproportionation :

$$SCl_2 \rightleftharpoons S_2Cl_2 \rightleftharpoons S_3Cl_2 \rightleftharpoons S_nCl_2 \rightleftharpoons S_8 + Cl_2$$

IV-4 SULPHUR AS A LIGAND IN METAL COMPLEXES :

Max. Schmidt [68] was able to form a six membered ring containing five sulphur atoms and one metal atom, where M = Ti. The two cyclopentadienyl rings complete the coordination of the Ti atom.

Complexes containing cyclic polysulphane chelating ligands often have strongly preferred ring sizes [69-71]. For the complexes Cp_2MS_5, where M = Ti, Zr and Hf, the ring size is six despite careful attempts to prepare smaller rings.
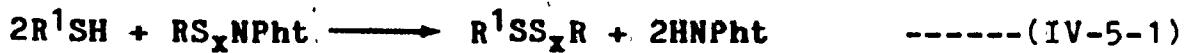
Polysulphide ligands have been structurally characterized in complexes such as Cp_2MoS_4 [72], Cp_2WS_4 [73], PtS_{15}^{-2} [74], $(PPh_3)_3PtS_4$ [75], Cp_2TiS_5 [76],

CpCo(PMe$_3$)S$_5$ [77], and Cp$_2$VS$_5$ [78]. The synthesis of trisulphanes with transition metals was unreported.
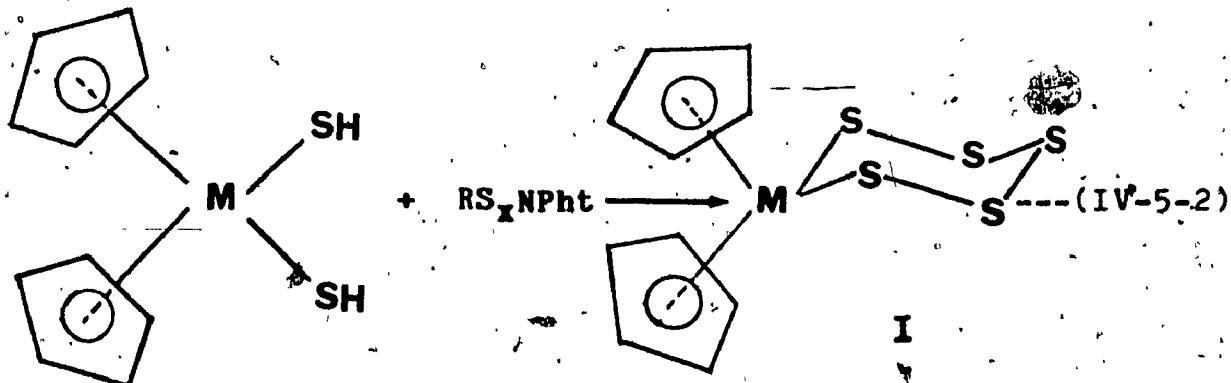
IV-5 REAGENTS FOR SULPHUR CHAIN FORMATION :

Many sulphur transfer reagents have been used to yield Organometallic compounds containing catenated sulphur as a ligand.
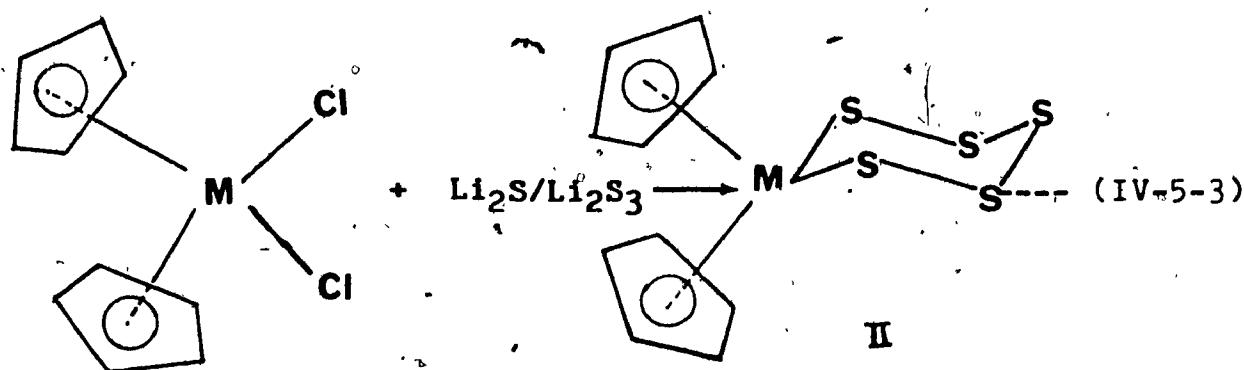
Sulphur transfer reagents of the type RS$_x$Npht where Npht = Phthalamide, x = 1 and 2, and R is an organic group provide an efficient route to unsymmetrical organic polysulphanes by reaction with thiols. [79]

$$2R^1SH + RS_xNPht \longrightarrow R^1SS_xR + 2HNPht \qquad \text{------(IV-5-1)}$$
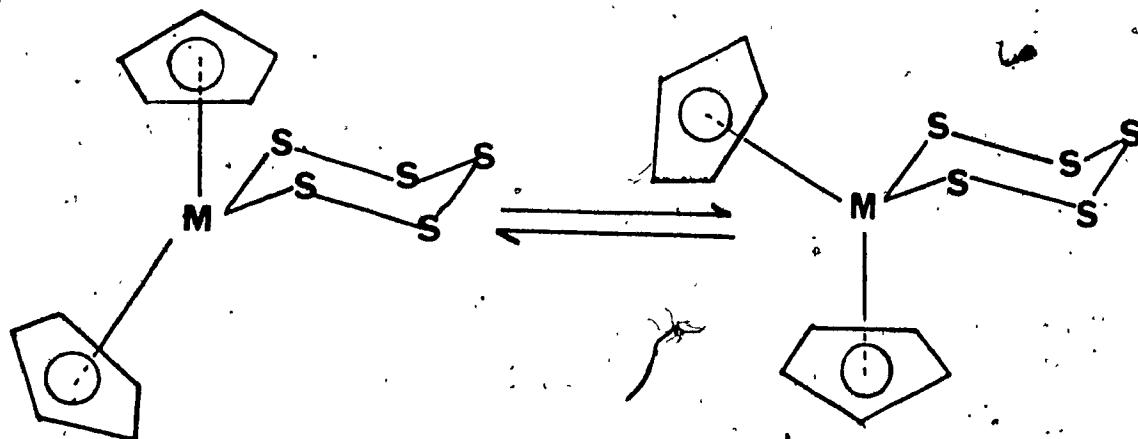
Similarly, Cp$_2$M(SH)$_2$ will react with the above reagents to give cyclic polysulphanes.

$$\text{------(IV-5-2)}$$

Anhydrous lithium polysulphides, have also been exploited as sulphur transfer reagents for the formation of polysulphanes of the type Cp_2MES ($E = S$, Se ; $M = Ti$, Hf, Zr) from the dichloro precursors :

$$+ \quad Li_2S/Li_2S_3 \longrightarrow \qquad \qquad \text{(IV-5-3)}$$

II
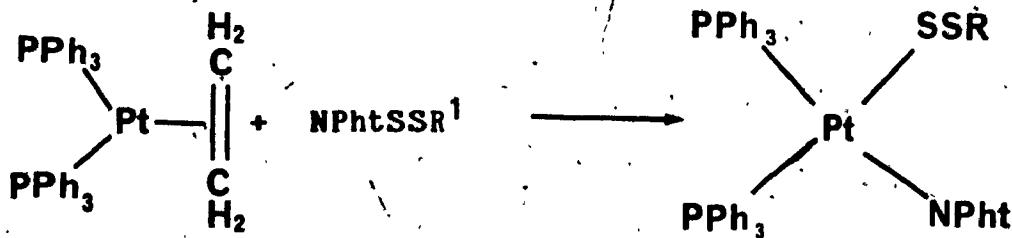
The compounds I and II were found to be air stable. Their N.M.R. spectra displayed variation with temperature :

At low temperature ^1H N.M.R. two peaks are observed and a chair to chair interconversion of Cp_2MS_5 species takes place, but as the temperature is increased the two peaks collapse to a singlet.

IV-6 $Pt(C_8H_4NO_2)SSCH(CH_3)_2(PPh_3)_2$:

Sulphur transfer reagents of the type RS_xNpht oxidatively add to platinum in the complex $(PPh_3)_2Pt(C_2H_4)$ to give the first platinum disulphanes :

Where $R = CH(CH_3)_2$, $CH_2CH_2CH_3$, $CH_2C_6H_5$, $p-C_6H_4CH_3$, NPht.

While most disulphanes tend to slowly lose sulphur upon standing in solution and could not be isolated by chromatography, the Pt-disulphanes obtained directly by the above reaction do not lose sulphur in this way.

The route to catenated sulphur complexes of platinum exploits a type of reactivity previously unreported

82

for the sulphur-nitrogen bond in the sulphur transfer reagents.

The presence of sulphur-phthalimide linkage in the complexes cis-(PPh$_3$)$_2$PtNPht(S$_x$NPht), where x = 1 and 2 promoted their treatment with thiols and thiolate anions in an attempt to extend the catenation. This was successful for the complex where x = 1. The Phthalamide sulphur bond is less reactive in the complexes than in the original sulphur transfer reagents.[82]

CRYSTAL DATA :

Given the novel nature of the Pt-S-S-R group it was decided to investigate the crystal structure so that its precise geometry could be established. By making a comparison with the similar groups some insight into the factors influencing metal-sulphur chain stability might eventually be achieved.

The crystal studied was a thick yellow plate with dimensions 0.5 x 0.4 x 0.1 mm. Zero and first level Weissenberg and Precession photographs were used to check crystal quality and provide preliminary information about the space group and unit cell dimensions. The systematic absences for hol; l = 2n+1, and oko; k = 2n+1 define the space group to be P 2$_1$/c.

The cell dimensions a = 11.963(4)Å , b = 17.382(5)Å , c = 22.030(8)Å , β = 115.28(3)° , V = 4141.9Å , Z = 4 were obtained on the diffractometer. Thus, 20 reflections were centered at both +ve and -ve 2θ values and averaged 2θ , ω , χ and ϕ angles were used in the refinement.

The structure was solved using a three dimensional Patterson synthesis which revealed the position of the heavy Pt atom. For P 2_1/c, the co-ordinates of equivalent position in the real cell are x,y,z; -x,-y,-z; -x,1/2+y,1/2-z; x,1/2-y,1/2+z, whereas, Patterson peaks are present at :

(i)	0,0,0	x 4	
(ii)	+2x,1/2,1/2+2z	x 2	(Harker Section)
(iii)	0,1/2+2y,1/2	x 2	(Harker Line)
(iv)	+2x,+2y+2z	x 1	
(v)	+2x,-2y,+2z	x 1	

On the Harker section, a peak is present at 0.153, 0.50, 0.1998 and on the Harker line at 0.0, 0.1375, 0.500, which yielded the position of the Pt atom at x = 0.153, y = 0.1375, z = 0.1998. To check, look for the peak at : 2x = 0.306, 2y = 0.275, 2z = 0.6040 and it was present at (iv).

The remaining non-hydrogen atoms were located on Fourier syntheses. The structure was refined isotropically and then anisotropically by using block diagonal least square matrices. After 5 cycles of least-squares refinement the residuals converged to R = 5.5% and Rw = 9.2% for the 4347 reflections in the range $3.5° < 2\theta < 45°$ (MoKα, $\underline{\lambda}$ = 0.7107Å) with I > 3σ(I).

DESCRIPTION OF THE STRUCTURE :

The geometry around the Pt atom was found to be square planar. (Fig.IV-6-2). The bond lengths in the Pt co-ordination sphere are Pt-P$_1$ = 2.265(3)Å, Pt-P$_2$ = 2.295(3)Å, Pt-N = 2.044(9)Å Pt-S$_1$ = 2.353(3)Å. The P$_1$-Pt-P$_2$ angle is 98.4(1)° . The geometry deviates from perfect square planar configuration due to the presence of bulky triphenyl phosphine groups present around platinum : the two triphenyl phosphine groups show normal bond lengths and bond angles internally .

The bond distances and bond angles are listed in Table IV-6-1 , and positional co-ordinates of the atoms are listed in Table IV-6-2.

A comparison of the bond angles and bond distances around similar square planar platinum complexes has been summarized in Table 1.

85

TABLE 1 : [83-87] <u>MOLECULAR PARAMETERS AROUND SQUARE PLANAR</u>
<u>PLATINUM</u> :
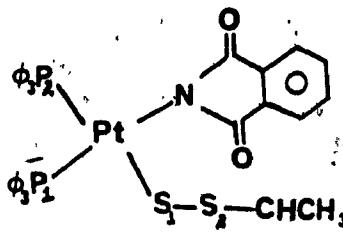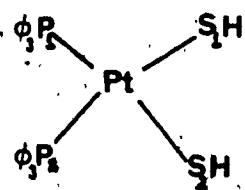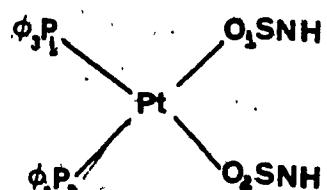
COMPLEXES	BOND DISTANCES(Å)	BOND ANGLES($^\circ$)
	$\text{Pt-P}_1 = 2.265(3)$ $\text{Pt-P}_2 = 2.295(9)$ $\text{Pt-N} = 2.044(9)$ $\text{Pt-S}_1 = 2.353$	$\text{P}_1\text{-Pt-P}_2 = 98.40(1)$ $\text{P}_1\text{-Pt-S}_1 = 85.41(1)$ $\text{S}_1\text{-Pt-N} = 89.70(3)$ $\text{P}_2\text{-Pt-N} = 86.9(3)$
	$\text{Pt-P}_1 = 2.286(2)$ $\text{Pt-P}_2 = 2.279(2)$ $\text{Pt-S}_1 = 2.340(2)$ $\text{Pt-S}_2 = 2.340(2)$	$\text{P}_1\text{-Pt-P}_2 = 97.65(7)$ $\text{S}_1\text{-Pt-P}_1 = 89.27(7)$ $\text{S}_2\text{-Pt-P}_2 = 90.06(8)$ $\text{S}_1\text{-Pt-S}_2 = 83.14(8)$
	$\text{Pt-P}_1 = 2.288$ $\text{Pt-P}_2 = 2.261$ $\text{Pt-O}_1 = 2.173$ $\text{Pt-O}_2 = 2.088$	$\text{P}_1\text{-Pt-P}_2 = 98.0$ $\text{P}_1\text{-Pt-O}_1 = 85.1$ $\text{O}_1\text{-Pt-O}_2 = 86.0$ $\text{O}_2\text{-Pt-P}_2 = 90.8$

Table 1 continued :
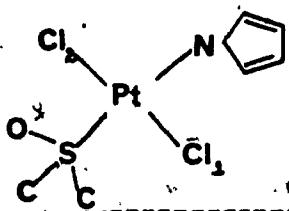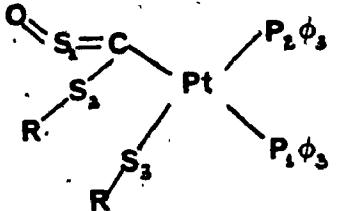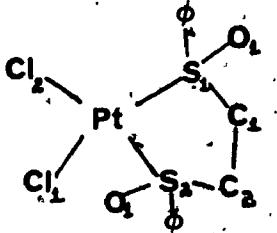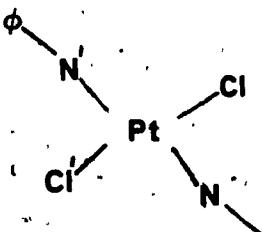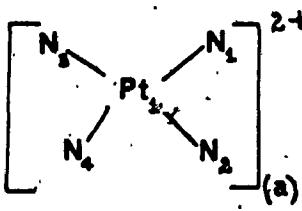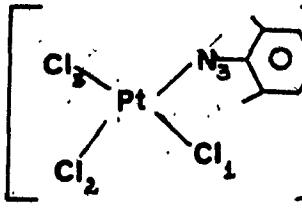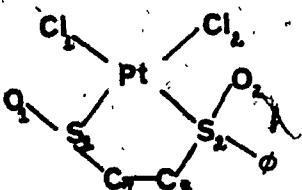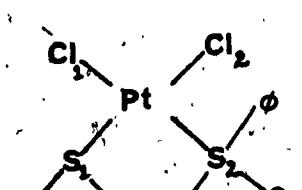
COMPLEXES	BOND DISTANCES(Å)	BOND ANGLES($^\circ$)
	Pt-N $= 2.05$	Cl_1-Pt-N $= 89.6$
	Pt-S $= 2.224$	N-Pt-Cl_2 $= 87.3$
	Pt-$Cl_1= 2.299$	Cl_2-Pt-S $= 93.4$
	Pt-$Cl_2= 2.276$	S-Pt-Cl_1 $= 89.7$
	Pt-$P_1 = 2.337(3)$	P_1-Pt-P_2 $= 96.9(1)$
	Pt-$P_2 = 2.287(3)$	P_1-Pt-S_3 $= 82.6(1)$
	Pt-$S_3 = 2.379(4)$	P_2-Pt-C $= 89.3(4)$
	Pt-C $= 2.01(1)$	C-Pt-S_3 $= 91.7(4)$
	Pt-S_1 $= 2.195$	
	Pt-S_2 $= 2.203$	
	Pt-$Cl_1= 2.308$	
	Pt-$Cl_2= 2.326$	
	Pt-Cl $= 2.302$	N-Pt-Cl $= 94.6$
	Pt-N $= 2.078$	N'-Pt-Cl $= 85.4$

Table 1 continued :

COMPLEXES	BOND DISTANCES(Å)	BOND ANGLES($^\circ$)
(a)	$Pt-N_1 = 2.052(7)$ $Pt-N_2 = 2.057(5)$	$N_1-Pt_1-N_2 = 89.7$ $N_1-Pt_1-N_2 = 90.3$
(b)	$Pt-Cl_1 = 2.302(2)$ $Pt-Cl_2 = 2.303(2)$ $Pt-Cl_3 = 2.309(2)$ $Pt-N_3 = 2.024(5)$	$Cl_1-Pt_2-Cl_3 = 90.5$ $Cl_2-Pt_2-Cl_3 = 92.2$ $Cl_2-Pt_2-N_3 = 89.1$ $Cl_1-Pt_2-N_3 = 89.1$
	$Pt-Cl_1 = 2.318(3)$ $Pt-S_1 = 2.217(2)$ $Pt-S_2 = 2.209(3)$ $Pt-Cl_2 = 2.313(2)$	$Cl_1-Pt-S_1 = 89.20$ $S_1-Pt-S_2 = 89.40$ $S_2-Pt-Cl_2 = 89.43$ $Cl_2-Pt-Cl_1 = 92.67$
	$Pt-Cl_1 = 2.295(4)$ $Pt-Cl_2 = 2.305(5)$ $Pt-S_1 = 2.192(4)$ $Pt-S_2 = 2.188(4)$	$Cl_1-Pt-Cl_2 = 91.9$ $Cl_1-Pt-S_1 = 88.7$ $S_1-Pt-S_2 = 89.7$ $S_2-Pt-Cl_2 = 90.4$

88

The Pt-S distance of 2.353Å falls in the same range as that found in [trans-dichloro(DMSO)(pyridine)PtII], 2.224Å [83]; [cis-(PPh$_3$)$_2$(SH)$_2$Pt], 2.360(2)Å, 2.340(2)Å [84], [cis-[PtCl$_2$](meso-PhSOCH$_2$CH$_2$-SOPh)], 2.217(2)Å and 2.209(3)Å [85], but is significantly longer than found in cis-[rac-cis1,2,bis(Phenylsulphinyl)ethylene dichloro PtII], 2.195Å [86] and cis-[PtCl$_2$(rac-cis-PhSOCH=CHSOPh)], 2.198Å [87]. In summary, the Pt-S distance is similar to that for other simple thiolate ligands. [88]

The Pt-N distance of 2.044(9)Å agrees well with the trans-[dichloro DMSO (pyridine)PtII], 2.05Å [89], bis (2-amino ethanol)di-iodoPtII), 2.06Å[90], [trans dichloro bis(cyclohexylamine)PtII], 2.078Å [91], [tetramine PtII bis-trichloro(2,6,dimethyl pyridine platinate(II)], 2.052(7), 2.057(3), 2.024(2)Å [92].

In addition to this the Pt-N bond length of 2.044Å is in good agreement with the published data on Pt-amine compounds. [93-94]
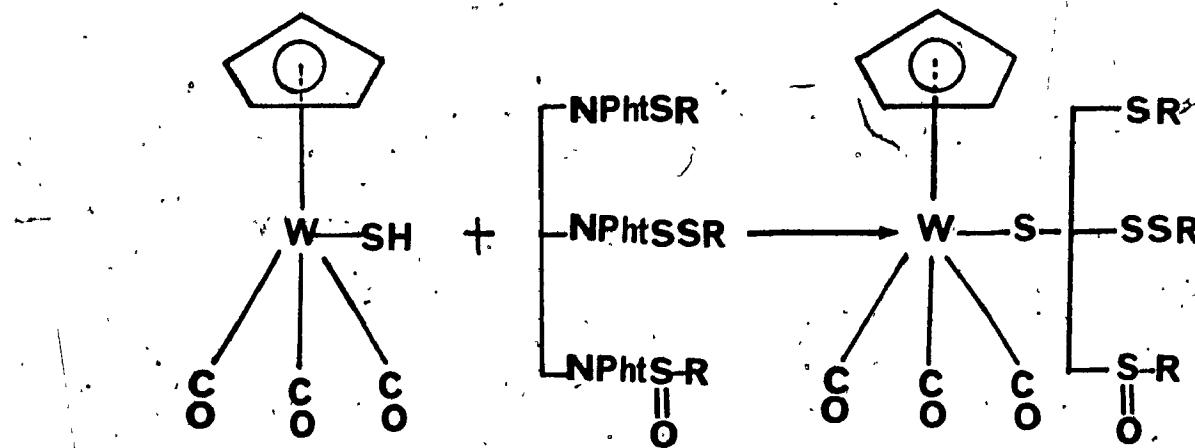
The S-S bond length of 2.037(4)Å is in the same range as found for the most organic and inorganic compounds. [95-96], but differs slightly from S$_6$ and S$_8$ bond distances of 2.06Å.

The most interesting feature observed in the complex is the Pt-S-S-R moiety in which the torsion angle is 89.4°. A discussion and comparison of torsion angle with

other complexes is deferred until later.

IV-7 $(\eta^5-C_5H_5)W(CO)_3-S-S-p-C_6H_4CH_3$:

The reaction of sulphur transfer reagents of the type RS_xNPht (NPht = phthalimide group, X = 1,2, R = Organic group) with tungsten thiol complexes $CpW(CO)_3SH$, where, Cp = $\eta^5-C_5H_5$ led to the formation of tungsten disulphanes. [97].

Tungsten disulphane complexes are stable in the solid state but slowly lose sulphur in solution. Many attempts were made to prepare trisulphanes but they decomposed to complicated mixtures upon workup. The tungsten

polysulphanes are less stable than organic di- and trisulphanes, however the oxidized tungsten disulphanes are more stable than organic analogues RSSOR [98].

As for the Pt complex, the primary purpose of the crystal structure determination was an interest in the geometry of the M-SS-R linkage.

CRYSTAL DATA :

The crystal studied was of red colour having a brick like shape. Preliminary Weissenberg and Precession photographs showed 2/m Laue symmetry and systematic absences which limited the possible space groups to P 2_1/c. Accurate cell dimensions obtained on a fully automated Picker FACS-1 four circle diffractometer equipped with a graphite monochromator and coupled to PDP/8a minicomputer were a = 10.640(3), b = 11.400(3), c = 12.872(3)Å, β = 94.58(2), Z = 4, V = 1556.3 Å.

The structure was solved by "heavy atom" methods using 1672 reflections with I>3σ(I) collected in the range 3.5° <2θ <45.0° . The heavy atom method located the position of the W atom. For P 2_1 /c the Patterson peaks are present at :

(i)   0,0,0   x 4

(ii) +2x,1/2,1/2+2z   x 2   (Harker Section)

(iii) 0,1/2+2y,1/2   x 2   (Harker Line)
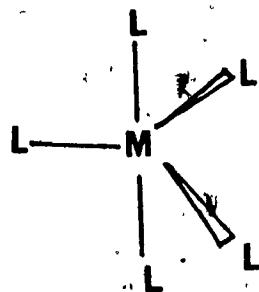
(iv) +2x,+2y,+2z   x 1

(v) +2x,-2y,+2z   x 1.

On the Harker section,a peak is present at 0.1596,0.5, -0.2155 and on the Harker line, at 0.0, - 0.1528, 0.500, which yields the position of the W atom at x = 0.1596, y = 0.1582, z = 0.2155. To check look for the peak at : 2x = 0.3192, 2y = 0.3164, 2z = 0.4310 and it was found at (iv).
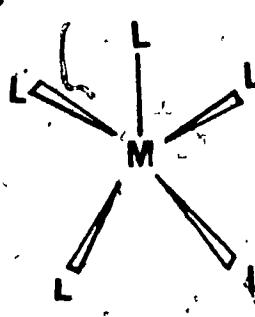
The positions of the other non-hydrogen atoms were found using a Fourier electron density map. The structure was refined isotropically and later by block diagonal least squares procedures using anisotropic thermal parameters but neglecting contributions from hydrogen atoms. The final unweighted and weighted discrepancy factors were RF = 4.0%, RwF = 5.5%.

DESCRIPTION OF THE STRUCTURE :

Tungsten, being divalent (d^4 system), has five co-ordinating ligands. There are two possible geometries proposed for the metal with co-ordination No.5. These two structures do not differ much in energy, therefore, one can be converted into other by very small changes in bond angles. For this reason many 5 co-ordinate complexes do not have either structure but a structure which is intermediate between these two.

Trigonal bipyramidal   Square pyramidal

The bond distances around the W atom are as follows :
$W-C_1$ = 1.928(10)Å, $W-C_2$ = 1.989(10)Å, $W-C_3$ = 1.954(10)Å, $W-S_1$ = 2.506(2)Å, $W-C_{av}$ = 2.342(9)Å .

A comparison of bond distances and bond angles of carbonyl and cyclopentadienyl derivatives of tungsten are shown in Table II [99-110] and interestingly, not much deviation is observed.

The W-S bond length of 2.506(2)Å is approximately the same as found in $[W_3OS_8(H_2O)]^{-2}$, 2.45Å [111] $(C_4H_8S)Cl_2W(\mu-S)(\mu-SEt)_2WCl_2(SC_4H_8)$, 2.442(3)Å [112] but is significantly longer than in $(Ph_4P)_2[(S_5)FeS_2WS_2]$, $W-S_t$ = 2.156(3)Å and $W-S_b$ = 2.247(10)Å [113], in $(PPh_3)(CH_2Ph)[WCl_5S]$ for the anion $[WCl_5S]$ 2.132(13)Å [114]

The S-S bond length of 2.053(4)Å in W-S-S-R is in the same range found for most organic and inorganic compounds. [115-116].

Table 2 MOLECULAR PARAMETERS FOR CARBONYL AND CYCLOPENTADIENYL DERIVATIVES OF TUNGSTEN :

COMPLEXES	DISTANCES($\AA$)				ANGLES($^{\circ}$)
	W-C_5H_5 (Cent)	W-C_5H_5 (ring)	W-C (carb)	C-O	W-C-O
$(\eta^5-C_55H_5)W(CO)_3SSR$	--	2.340	1.957	1.163	176.9
$[(C_5H_5)W(CO)_3]_2$	--	2.340	1.976	1.149	175.2
$[(C_5H_5)W(CO)_3Au(PPh_3)]$	2.01	2.362	1.970	1.161	172.0
$[(C_5H_5)W(CO)_3PH]$	--	--	1.960	1.180	168.0
$[(C_4H_{10}S_2)W(CO)_3Cl(SnMeCl_2)]$	--		1.96	1.16	175.0
$[(C_{10}H_8N_2)W(CO)_3Br(GeBr_3)]$	--		1.91	1.19	171.0
$[(C_5H_5)_2WS_4]$	2.01	--	--	--	--
$[(C_6H_4)(SMe)_2W(CO)_4]$	--	--	2.00	1.13	167.0

<u>Table II</u> <u>cotinued</u> :
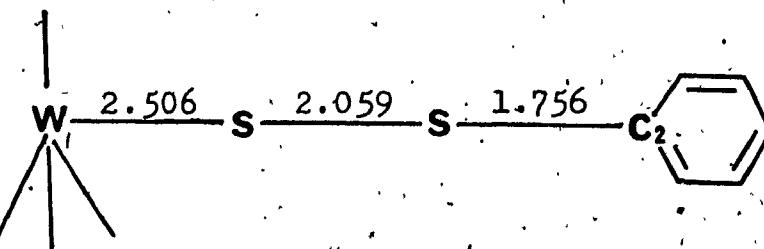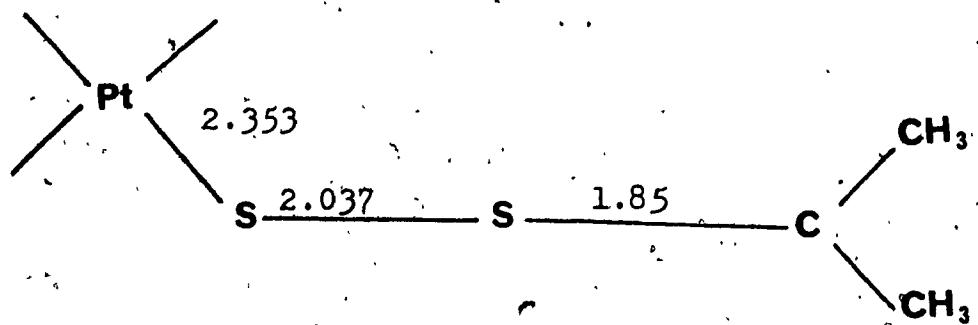
COMPLEXES	DISTANCES(Å)				ANGLES(°)
	W-C_5H_5 (Cent)	W-C_5H_5 (ring)	W-C (Carb)	C-O	W-C-O
[Et_4N][$W(CO)_4Br_3$]	--	--	1.96	1.15	--
[$(Ph_2C_2)_3W(CO)$]	--	--	1.99	1.16	--
[{$(C_5H_5)W(CO)_3(AlMe)_2$}$_2$]	2.016	--	1.97 1.85(1)	1.19	173.0
[{$(C_5H_5)W(CO)_3$}$_3Al$]$3C_4H_8$	2.04	--	1.95 1.85(1)	1.16	176.0
[$W(CO)_4(CNC_6H_{11})CS$]	--	--	2.064	1.104- 1.155	176.2- 179.3
[$(C_5H_5)W(CO)_3Cl$]	2.001	2.326	1.99	1.139	177.3
[{$(C_5H_5)W(CO)_3$}GaC_9H_6]	2.00	2.35	1.96	--	175.0

95

COMPARISON OF THE M-SS-R LINKAGE IN Pt AND W :

Take into consideration only the metal and the sulphur moiety of the two complexes and compare :

Pt — S : 2.353

S —2.037— S —1.85— C

C(CH₃)(CH₃):

$$Pt \xrightarrow{2.353} S \xrightarrow{2.037} S \xrightarrow{1.85} C \begin{array}{c} CH_3 \\ CH_3 \end{array}$$

$$W \xrightarrow{2.506} S \xrightarrow{2.059} S \xrightarrow{1.756} C_2 \text{(aromatic ring)}$$
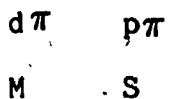
In the case of the Pt complex(I) the torsion angle of 89.5° is observed whereas, in the case of W complex(II) it is 63.1° . The large variation in the dihedral angle might be accounted for by the steric effect due to the aromatic ring in the case of the tungsten complex. Also, a bond is formed by the dπ orbital of metal and dπ orbital of

sulphur atom.

$d\pi \quad d\pi$

$M \quad S$

Whereas, back bonding takes place from the $p\pi$ orbitals of sulphur atom to metal $d\pi$ orbitals :

$d\pi \quad p\pi$

$M \quad S$
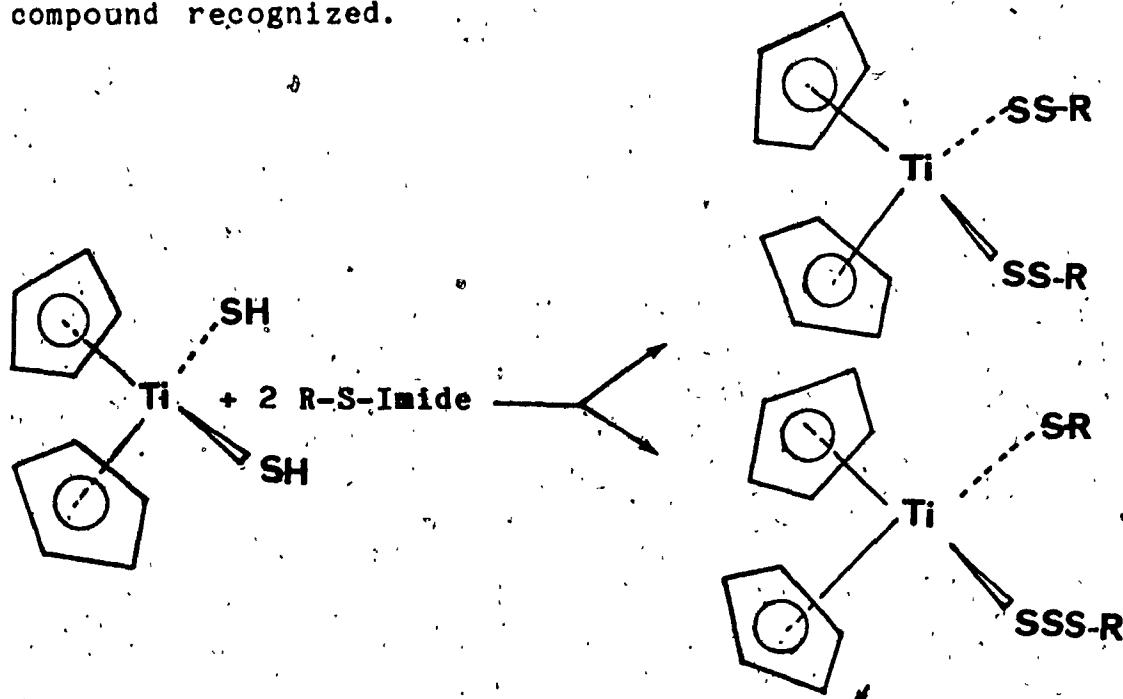
Due to this, some change in the lone pair distribution on the sulphur atom is expected resulting in a change in the torsion angle. The relative contributions of these effects can not be easily evaluated.

It appear that dihedral angle falls in the range $80°-90°$ for the unstrained disulphides and the value of torsion angle will be less for the strained complex [117.]

IV-8 $[(\eta^5-C_5H_5)_2Ti(SSSC_6H_5)SC_6H_5]$:

The complex $Cp_2Ti(SH)_2$ was treated with two equivalents of RSImide, where Imide = Phthalamide; R = $CHMe_2$, p-$C_6H_4CH_3$ and Imide = succinimide; R'= C_6H_5, to give the symmetrical disulphane $Cp_2Ti(SSR)_2$ when R = $CHMe_2$ and the unsymmetrical trisulphanes $Cp_2Ti(SR)(SSSR)$ when R = C_6H_5 and p-$C_6H_4CH_3$. Examples of metallo trisulphane [119] are rare, and the presence of this grouping was not suspected. The crystal structure determination of the compound expected to be a symmetrical disulphide was initiated, to add a further example to the range of known structures. Only during the structure solution was the true nature of the compound recognized.

II-1 R = $CHMe_2$, III-2 R = p-C_6H_4Me, III-3 R = C_6H_5.

CRYSTAL DATA :

The crystal of $[(\eta^5 - C_5H_5)_2Ti(SSSC_6H)SC_6H_5]$ was red with a brick like shape. The crystal system was monoclinic and systematic absences define the space group $P 2_1/c$. The lattice constants obtained on the four circle diffractometer were a = 7.794(5), b = 14.664(10), c = 18.360(10)Å, β = 101.90(6)$^\circ$, Z = 4 V = 2053.3Å, d_{cal} = 1.490g cm^{-3}. A hemishere of 3783 reflections measured on a Picker FACS-1 automated diffractometer yielded 1912 independent reflections. The structure was solved by direct methods using 100 reflections with E>1.7 and was refined by block-diagonal least square procedures. The structure was refined isotropically and later anisotropically, 6 cycles of least-squares refinement converged the residual factor to R = 3.7% and Rw = 5.0%. Hydrogen atoms were included in the calculated positions.

DESCRIPTION OF THE STRUCTURE :

In $[(\eta^5 - C_5H_5)_2Ti(SSSC_6H_6)SC_6H_6]$ there is a difference in the two Titanium-Sulphur distances Ti-S$_1$ = 2.439(3)Å ; Ti-S$_4$ = 2.381(3)Å, but this may not be entirely due to its unsymmetrical structure since similar asymmetry was observed for Cp$_2$V(SPh)$_2$ [120]. The two S-S distances , S$_1$-S$_2$ = 2.053(3), S$_2$-S$_3$ = 2.011(3)Å are within the ranges

observed for trisulphides and variation between them is presumably a consequence of different subsituents terminating the S_3 chains.

The $S_1-S_2-S_3$ angle of 109.3(1)$^\circ$ is also within the ranges observed for trisulphides [121].

The torsion angle between $Ti-S_1-S_2-S_3$ is 70.443° and between $S_1-S_2-S_3-C_{21}$ is 78.976° [122].

The angles between $Ti-S_1-S_2, S_1-S_2-S_3$ and $S_2-S_3-C_{21}$ are 115.6(1)$^\circ$, 109.3(2)$^\circ$ and 106.3(4)$^\circ$ respectively. The non-bonded distances from S_4-S_1, S_4-S_2 and S_4-S_3 are 3.645, 4.352 and 3.838 Å respectively.

The geometry around Ti atom is some what distorted tetrahedral. The parameters around the co-ordination sphere of Titanium are $Ti-S_4$ = 2.381(3), $Ti-S_1$ = 2.439(3), $Ti-CNT1$ = 2.0491(1) and $Ti-CNT2$ = 2.0363(1) Å. The angles around Ti are shown below :
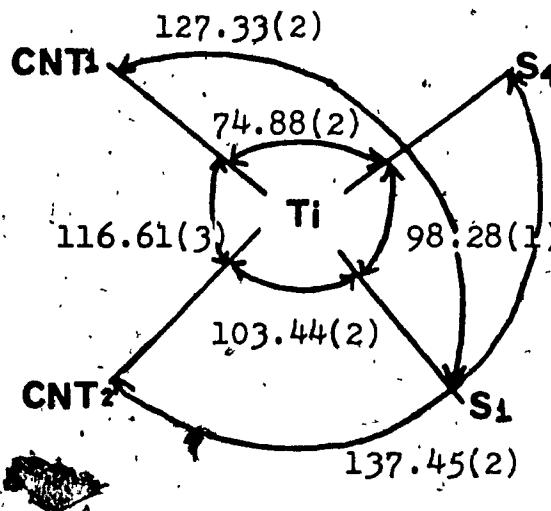
Fig.IV-6-1

The two cyclopentadienyl rings are π-bonded to the Ti atom. The rings are staggered with centroid to Ti distances of 2.0434(1) and 2.0363(1)Å. The average Ti-Cp carbon distances of 2.369Å is comparable to those found for similar complexes [123] of the type $(\eta^5-C_5H_5)_2TiX_2$ (X=Cl,S). The Cp-M-Cp angle in the complex under study is 132.55(4)°. This value falls in the same range as that obtained in Cp_2TiS_5(132.7)° , Cp_2MoS_4 (134.0)° , Cp_2VS_5(134.1)° , Cp_2WS_4(135.1)° , $[\eta^5-C_5(CH_3)_5]_2TiCl_2$ (137.4)° [124].

A list of bond distances and angles, and list of positional co-ordinates are given in Table IV-8-5 and Table IV-8-6 respectively.

Table IV-6-1   Distances and Angles in $C_{47}H_{41}NO_2P_2PtS_2$

Distances

Pt-P1	2.265(3)	S1-S2	2.037(4)
Pt-P2	2.295(3)	S2-C11	1.85(1)
Pt-S1	2.353(3)	C11-C12	1.56(2)
Pt-N	2.044(9)	C11-C13	1.52(2)
P1-C111	1.84(1)	P2-C211	1.80(1)
C111-C112	1.39(2)	C211-C212	1.40(2)
C111-C116	1.36(2)	C211-C216	1.38(2)
C112-C113	1.42(2)	C212-C213	1.37(2)
C113-C114	1.37(2)	C213-C214	1.39(2)
C114-C115	1.40(2)	C214-C215	1.38(2)
C115-C116	1.40(2)	C215-C216	1.43(2)
P1-C121	1.81(1)	P2-C221	1.81(1)
C121-C122	1.38(2)	C221-C222	1.39(2)
C121-C126	1.44(2)	C221-C226	1.36(2)
C122-C123	1.39(2)	C222-C223	1.42(2)
C123-C124	1.39(2)	C223-C224	1.37(2)
C124-C125	1.43(2)	C224-C225	1.38(3)
C125-C126	1.36(2)	C225-C226	1.43(2)
P1-C131	1.81(1)	P2-C231	1.83(1)
C131-C132	1.37(2)	C231-C232	1.38(2)
C131-C136	1.43(2)	C231-C236	1.37(2)
C132-C133	1.42(2)	C232-C233	1.38(2)
C133-C134	1.32(2)	C233-C234	1.42(2)
C134-C135	1.42(2)	C234-C235	1.42(2)
C135-C136	1.35(2)	C235-C236	1.44(2)
N-C1	1.36(1)	N-C2	1.36(1)
C1-O1	1.18(1)	C4-C5	1.36(2)
C1-C3	1.47(2)	C5-C6	1.44(2)
C3-C4	1.36(2)	C6-C7	1.36(2)
C2-C4	1.53(2)	C7-C8	1.42(2)
C2-O2	1.20(1)	C8-C3	1.41(2)

Table IV-6-1

Angles

P1-Pt-P2	98.4(1)	P2-Pt-S1	175.0(1)
P1-Pt-S1	85.4(1)	P2-Pt-N	86.9(3)
P1-Pt-N	171.4(3)	S1-Pt-N	89.7(3)
Pt-P1-C111	114.1(4)	Pt-P2-C211	112.7(4)
Pt-P1-C121	108.7(4)	Pt-P2-C221	113.8(4)
Pt-P1-C131	118.5(4)	Pt-P2-C231	113.4(4)
C111-P1-C121	104.1(5)	C211-P2-C221	104.1(5)
C111-P1-C131	102.6(5)	C211-P2-C231	108.9(5)
C121-P1-C131	107.7(5)	C221-P2-C231	103.2(5)
C116-C111-C112	122.1(11)	C216-C211-C212	119.2(11)
C111-C112-C113	116.5(13)	C211-C212-C213	121.2(11)
C112-C113-C114	122.0(13)	C212-C213-C214	121.0(12)
C113-C114-C115	119.4(12)	C213-C214-C215	118.4(12)
C114-C115-C116	119.1(13)	C214-C215-C216	121.2(12)
C115-C116-C111	120.6(12)	C215-C216-C211	118.9(11)
C116-C111-P1	118.7(9)	C216-C211-P2	116.9(9)
C112-C111-P1	118.8(9)	C212-C211-P2	123.8(9)
C216-C121-C122	118.9(11)	C226-C221-C222	120.0(12)
C121-C112-C123	121.2(12)	C221-C222-C223	119.9(14)
C122-C123-C124	119.5(12)	C222-C223-C224	118.2(16)
C123-C124-C125	120.2(12)	C223-C224-C225	123.6(15)
C124-C125-C126	119.6(14)	C224-C225-C226	116.6(15)
C125-C126-C121	120.6(13)	C225-C226-C221	121.4(13)
C126-C121-P1	120.8(9)	C226-C221-P2	121.0(9)
C122-C121-P1	120.3(9)	C222-C221-P2	119.0(10)
C136-C131-C132	117.4(11)	C236-C231-C232	123.5(11)
C131-C132-C133	120.7(12)	C231-C232-C233	119.1(12)
C132-C133-C134	119.6(13)	C232-C233-C234	119.5(12)
C133-C134-C135	122.2(14)	C233-C234-C235	121.8(12)
C134-C135-C136	117.5(15)	C234-C235-C236	116.5(13)
C135-C136-C131	122.4(13)	C235-C236-C237	119.5(12)
C136-C131-P1	121.8(9)	C236-C231-P2	118.5(9)
C132-C131-P1	120.8(9)	C232-C231-P2	117.8(9)
Pt-N-C1	127.6(7)	C2-C4-C5	129.0(11)
Pt-N-C2	119.7(8)	C2-C4-C3	105.2(9)
C1-N-C2	112.0(9)	C3-C4-C5	125.7(11)
N-C1-O1	125.3(10)	C4-C5-C6	115.1(13)
N-C1-C3	106.8(9)	C5-C6-C7	121.0(13)
O1-C1-C3	127.7(10)	C6-C7-C8	121.8(13)
N-C2-O2	128.5(12)	C7-C8-C3	116.6(13)
N-C2-C4	106.9(10)		
O2-C2-C4	125.3(11)	Pt-S1-S2	111.6(2)
C1-C3-C8	130.8(11)	S1-S2-C11	103.6(4)

103

Table IV-6-1

C1-C3-C4	109.5(9)	S2-C11-C12	108.4(10)
C4-C3-C8	119.5(11)	S2-C11-C13	105.0(11)
		C12-C11-C13	113.0(12)

Table IV-6-2 TABLE OF ATOMIC PARAMETERS X,Y,Z AND BISO.
E.S.DS. REFER TO THE LAST DIGIT PRINTED.

	X	Y	Z	BISO
PT	0.15305(3)	0.137448(23)	0.802046(19)	2.578(16)
N	0.2589 (8)	0.1677 (5)	0.7535 (4)	3.0 (3)
C1	0.2234 (10)	0.2084 (6)	0.6955 (5)	2.9 (4)
O1	0.1205 (7)	0.2261 (5)	0.6598 (4)	4.3 (3)
C2	0.3831 (11)	0.1572 (8)	0.7842 (6)	3.8 (4)
O2	0.4422 (8)	0.1184 (5)	0.8324 (4)	4.3 (3)
C3	0.3366 (10)	0.2305 (7)	0.6897 (5)	3.3 (4)
C4	0.4364 (10)	0.2033 (7)	0.7432 (6)	3.6 (4)
C5	0.5562 (13)	0.2135 (9)	0.7547 (8)	5.2 (6)
C6	0.5753 (14)	0.2635 (9)	0.7081 (9)	5.8 (7)
C7	0.4781 (14)	0.2915 (9)	0.6533 (8)	5.5 (6)
C8	0.3542 (14)	0.2766 (9)	0.6417 (8)	5.6 (6)
P1	0.0615 (3)	0.10726 (17)	0.87017 (14)	2.81 (10)
C111	0.0060 (10)	0.1911 (6)	0.9005 (5)	3.1 (4)
C112	0.0278 (12)	0.1938 (9)	0.9676 (6)	4.0 (6)
C113	-0.0186 (14)	0.2591 (9)	0.9882 (8)	5.8 (6)
C114	-0.0908 (12)	0.3129 (8)	0.9435 (8)	5.3 (6)
C115	-0.1154 (12)	0.3059 (7)	0.8757 (8)	4.6 (5)
C116	-0.0664 (10)	0.2435 (7)	0.8552 (6)	3.6 (4)
C121	0.1755 (10)	0.0636 (7)	0.9459 (6)	3.3 (4)
C122	0.3001 (11)	0.0768 (7)	0.9655 (6)	3.9 (5)
C123	0.3892 (12)	0.0438 (8)	1.0236 (7)	4.8 (5)
C124	0.3526 (14)	-0.0059 (9)	1.0612 (7)	5.7 (6)
C125	0.2244 (15)	-0.0196 (12)	1.0424 (8)	7.5 (8)
C126	0.1384 (13)	0.0147 (11)	0.9866 (7)	6.1 (7)
C131	-0.0724 (10)	0.0452 (6)	0.8380 (6)	3.2 (4)
C132	-0.1890 (11)	0.0752 (7)	0.8061 (6)	4.0 (5)
C133	-0.2936 (12)	0.0263 (8)	0.7787 (8)	5.0 (6)
C134	-0.2784 (14)	-0.0490 (9)	0.7844 (9)	6.3 (7)
C135	-0.1605 (14)	-0.0834 (10)	0.8202 (10)	6.7 (8)
C136	-0.0617 (12)	-0.0364 (7)	0.8455 (8)	4.6 (6)
P2	0.1006 (3)	0.02883 (17)	0.73658 (14)	3.02 (10)
C211	0.1358 (10)	-0.0583 (7)	0.7854 (6)	3.2 (4)
C212	0.0621 (11)	-0.1245 (7)	0.7666 (6)	3.5 (4)
C213	0.0880 (12)	-0.1870 (7)	0.8085 (7)	3.9 (5)
C214	0.1915 (12)	-0.1878 (8)	0.8700 (6)	4.2 (5)
C215	0.2690 (12)	-0.1244 (8)	0.8876 (7)	4.2 (5)
C216	0.2416 (10)	-0.0582 (7)	0.8451 (6)	3.5 (4)
C221	0.1825 (11)	0.0185 (7)	0.6844 (6)	3.7 (4)
C222	0.1312 (15)	0.0499 (8)	0.6202 (7)	5.2 (6)
C223	0.1943 (17)	0.0430 (10)	0.5786 (9)	6.5 (8)
C224	0.3088 (16)	0.0098 (12)	0.6050 (8)	6.8 (8)
C225	0.3612 (15)	-0.0243 (10)	0.6675 (9)	6.3 (7)
C226	0.2953 (12)	-0.0163 (8)	0.7083 (7)	4.6 (5)
C231	-0.0623 (10)	0.0267 (7)	0.6758 (6)	3.4 (4)
C232	-0.1363 (11)	0.0874 (8)	0.6758 (6)	4.1 (5)
C233	-0.2573 (12)	0.0897 (8)	0.6277 (7)	4.7 (5)
C234	-0.3039 (13)	0.0285 (9)	0.5811 (7)	5.7 (6)
C235	-0.2286 (14)	-0.0344 (9)	0.5810 (7)	5.8 (6)
C236	-0.1016 (12)	-0.0322 (7)	0.6300 (6)	4.0 (5)
S1	0.2032 (3)	0.25495 (17)	0.86065 (15)	3.36 (10)
S2	0.3600 (3)	0.30169 (20)	0.86141 (16)	4.05 (12)
C11	0.4850 (11)	0.2593 (8)	0.9371 (7)	4.7 (5)
C12	0.4674 (14)	0.2866 (9)	1.0001 (7)	5.7 (6)
C13	0.6045 (14)	0.2884 (13)	0.9364 (9)	8.2 (9)

BISO IS THE ARITHMETIC MEAN OF THE PRINCIPAL AXES OF THE THERMAL

105

ELLIPSOID

Fig.IV-6-2

106
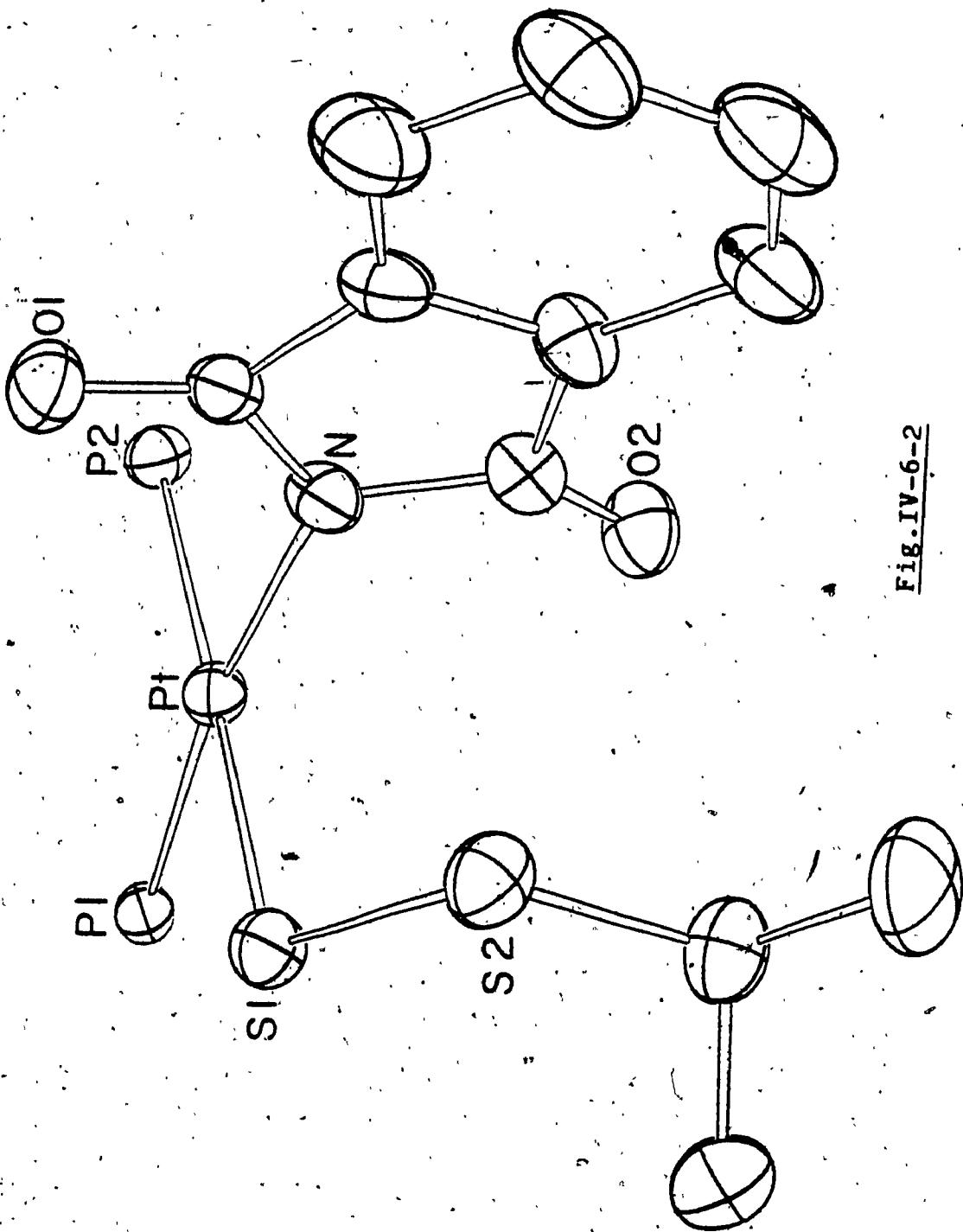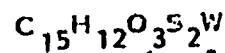
Table IV-7-3

Distances and Angles in $C_{15}H_{12}O_3S_2W$

Distances

W – Cl1	2.343(10)		W – C1	1.928(10)
W – Cl2	2.397(9)		W – C2	1.989(10)
W – Cl3	2.344(9)		W – C3	1.954(10)
W – Cl4	2.304(9)		W – S1	2.506(2)
W – Cl5	2.313(9)		S1 – S2	2.053(4)
S2 – C21	1.756(9)		C23 – C24	1.39(1)
C21 – C22	1.40(1)		C24 – C25	1.36(1)
C21 – C26	1.39(1)		C25 – C26	1.41(1)
C22 – C23	1.40(1)		C24 – C30	1.54(1)
C1 – O1	1.20(1)		C3 – O3	1.16(1)
C2 – O2	1.13(1)			
Cl1 – Cl2	1.45(1)		C13 – C14	1.40(1)
Cl1 – Cl5	1.38(1)		C14 – C15	1.45(1)
Cl2 – Cl3	1.41(1)			

Table IV-7-3

$C_{15}H_{12}O_3S_2W$

Angles

S1 – W – Cl1	98.6(3)	C13 – W – C14	35.1(4)
S1 – W – Cl2	80.7(3)	C13 – W – C15	58.7(3)
S1 – W – C13	100.0(3)	C13 – W – C1	97.8(4)
S1 – W – C14	134.9(2)	C13 – W – C2	155.7(4)
S1 – W – C15	132.9(3)	C13 – W – C3	120.0(4)
S1 – W – C1	80.0(3)		
S1 – W – C2	72.6(3)	C14 – W – C15	36.6(3)
S1 – W – C3	136.3(3)	C14 – W – C1	104.7(4)
		C14 – W – C2	143.7(4)
Cl1 – W – Cl2	35.7(3)	C14 – W – C3	87.4(4)
Cl1 – W – C13	58.9(4)		
Cl1 – W – C14	59.6(4)		
Cl1 – W – C15	34.1(4)	C15 – W – C1	139.2(4)
Cl1 – W – C1	156.3(4)	C15 – W – C2	108.9(4)
Cl1 – W – C2	98.6(4)	C15 – W – C3	86.1(4)
Cl1 – W – C3	116.1(4)		
		C1 – W – C2	103.4(4)
		C1 – W – C3	78.0(4)
Cl2 – W – C13	34.6(3)	C2 – W – C3	76.5(4)
Cl2 – W – C14	58.5(3)		
Cl2 – W – C15	57.9(3)	W – S1 – S2	113.3(1)
Cl2 – W – C1	122.0(4)	S1 – S2 – C21	104.1(3)
Cl2 – W – C2	121.5(4)	W – C1 – O1	176.7(8)
Cl2 – W – C3	142.7(4)	W – C2 – O2	176.3(9)
		W – C3 – O3	177.7(10)
C15 – Cl1 – C12	107.3(9)		
Cl1 – C12 – C13	107.2(9)		
C12 – C13 – C14	109.5(9)		
C13 – C14 – C15	106.3(9)		
C14 – C15 – Cl1	109.6(8)		
C26 – C21 – C22	120.3(8)		
C21 – C22 – C23	119.2(9)		
C22 – C23 – C24	120.9(9)		
C23 – C24 – C25	119.2(8)		
C24 – C25 – C26	121.6(9)		
C25 – C26 – C21	118.8(9)		

108

Table IV-7-4

TABLE OF ATOMIC PARAMETERS X,Y,Z AND BISO.
E.S.DS. REFER TO THE LAST DIGIT PRINTED.

	X	Y	Z	BISO
W	0.15944(3)	0.10829(3)	0.784734(25)	3.223(19)
S1	0.22355(22)	0.18521(21)	0.32986 (19)	4.09 (10)
S2	0.40220(22)	0.17257(25)	0.40209 (20)	4.61 (11)
C11	0.1046 (10)	0.3656 (9)	0.1063 (7)	4.2 (4)
C12	0.2370 (9)	0.3340 (9)	0.1225 (6)	4.2 (4)
C13	0.3027 (9)	0.4346 (10)	0.1608 (8)	4.6 (5)
C14	0.7818 (8)	0.0283 (9)	0.3341 (7)	4.1 (4)
C15	0.0952 (8)	0.4832 (9)	0.1291 (6)	4.2 (4)
C21	0.5002 (8)	0.2238 (8)	0.3084 (7)	3.7 (4)
C22	0.5043 (9)	0.1652 (9)	0.2133 (7)	4.2 (4)
C23	0.5814 (9)	0.2088 (8)	0.1394 (7)	4.3 (4)
C24	0.6587 (8)	0.3054 (8)	0.1615 (8)	4.3 (4)
C25	0.6538 (8)	0.3615 (10)	0.2547 (9)	4.3 (4)
C26	0.5741 (8)	0.3225 (8)	0.3299 (8)	4.3 (4)
C1	0.2707 (10)	0.4197 (8)	0.4079 (8)	4.5 (4)
C2	0.0118 (9)	0.3128 (8)	0.3397 (8)	4.3 (4)
C3	0.9267 (11)	0.0189 (9)	0.1481 (8)	5.2 (5)
01	0.3370 (8)	0.4424 (7)	0.4851 (6)	6.5 (4)
02	0.9239 (6)	0.2730 (7)	0.3693 (7)	6.6 (4)
03	0.9800 (11)	0.0915 (8)	0.1064 (8)	8.5 (6)
C30	0.7420 (12)	0.3538 (11)	0.0791 (9)	6.3 (6)

BISO IS THE ARITHMETIC MEAN OF THE PRINCIPAL AXES OF THE THERMAL

ELLIPSOID

Fig.IV-7-3

110
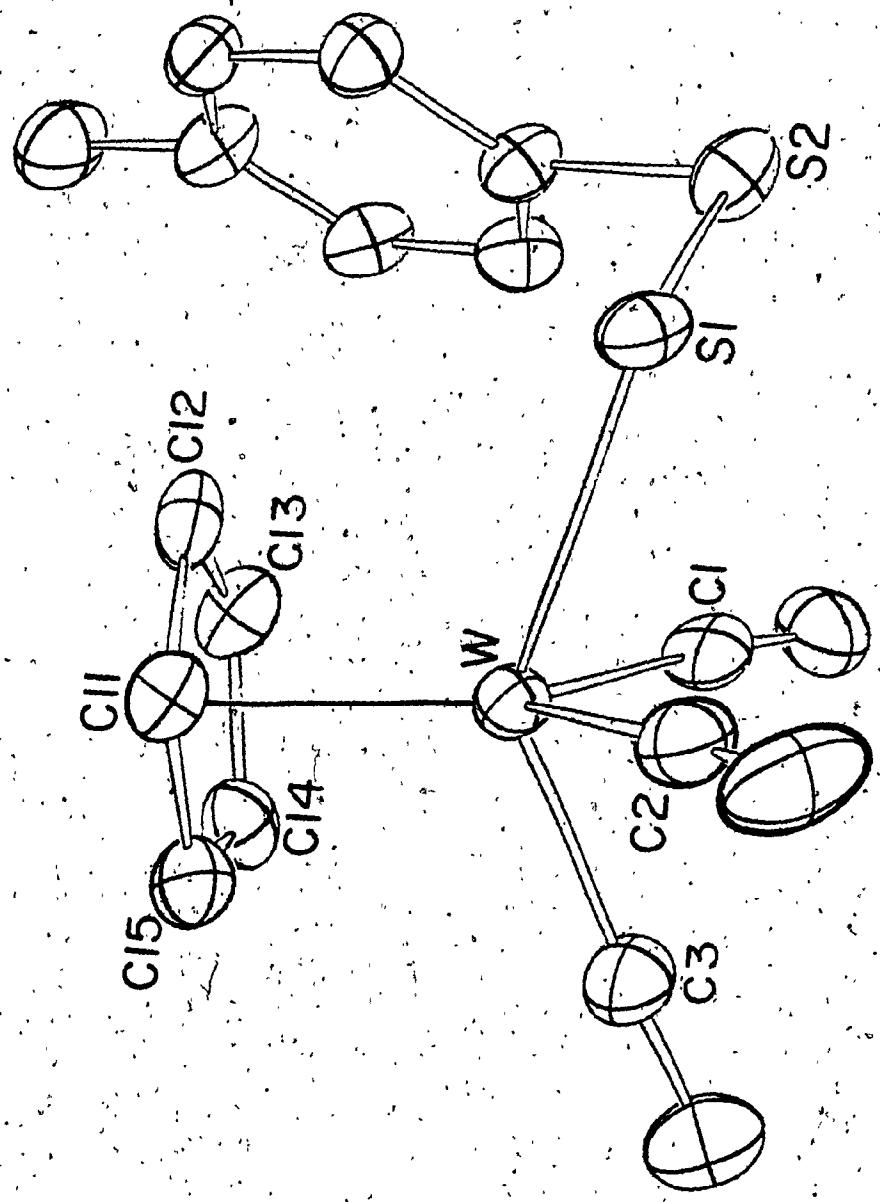
Table IV-8-5

Table 1. Distances and Angles in $(C_5H_5)_2Ti(SC_6H_5)(S_3C_6H_5)$ [a]

Distances

Atom 1		Atom 2	Distance (Å)		Atom 1		Atom 2	Distance
Ti	–	C(1)	2.365(6)		Ti	–	C(6)	2.363(7)
Ti	–	C(2)	2.346(7)		Ti	–	C(7)	2.353(7)
Ti	–	C(3)	2.365(7)		Ti	–	C(8)	2.349(7)
Ti	–	C(4)	2.385(6)		Ti	–	C(9)	2.355(7)
Ti	–	C(5)	2.374(7)		Ti	–	C(10)	2.352(7)
Ti	–	CNTR1 [b]	2.049(1)		Ti	–	CNTR2 [b]	2.0363(1)
Ti	–	S(1)	2.439(3)		S(1)	–	S(2)	2.053(3)
Ti	–	S(4)	2.381(3)		S(2)	–	S(3)	2.011(3)
S(3)	–	C(21)	1.755(7)		S(4)	–	C(11)	1.759(6)
C(21)	–	C(22)	1.388(11)		C(11)	–	C(12)	1.391(9)
C(21)	–	C(26)	1.361(11)		C(11)	–	C(16)	1.380(9)
C(22)	–	C(23)	1.389(11)		C(12)	–	C(13)	1.385(10)
C(23)	–	C(24)	1.354(14)		C(13)	–	C(14)	1.368(11)
C(24)	–	C(25)	1.357(16)		C(14)	–	C(15)	1.377(10)
C(25)	–	C(26)	1.404(13)		C(15)	–	C(16)	1.389(9)
C(1)	–	C(2)	1.39(1)		C(6)	–	C(7)	1.38(1)
C(2)	–	C(3)	1.39(1)		C(7)	–	C(8)	1.40(1)
C(3)	–	C(4)	1.38(1)		C(8)	–	C(9)	1.39(1)
C(4)	–	C(5)	1.40(1)		C(9)	–	C(10)	1.37(1)
C(5)	–	C(1)	1.40(1)		C(10)	–	C(6)	1.39(1)

Table 1 continued

Angles

Atom 1		Atom 2		Atom 3	Angle (deg)	Atom 1		Atom 2		Atom 3	Angle (deg)
CNTR1	–	Ti	–	CNTR2	132.55(–)	Ti	–	S(1)	–	S(2)	115.5(1)
CNTR1	–	Ti	–	S(1)	109.64(–)	S(1)	–	S(2)	–	S(3)	109.3(1)
CNTR1	–	Ti	–	S(4)	101.36(–)	S(2)	–	S(3)	–	C(21)	106.8(3)
CNTR2	–	Ti	–	S(1)	99.34(–)	Ti	–	S(4)	–	C(11)	114.5(2)
CNTR2	–	Ti	–	S(4)	110.88(–)						
S(1)	–	Ti	–	S(4)	98.3(1)						
C(1)	–	C(2)	–	C(3)	108.2(6)	C(6)	–	C(7)	–	C(8)	107.4(7)
C(2)	–	C(3)	–	C(4)	107.9(6)	C(7)	–	C(8)	–	C(9)	108.0(6)
C(3)	–	C(4)	–	C(5)	108.7(6)	C(8)	–	C(9)	–	C(10)	108.0(7)
C(4)	–	C(5)	–	C(1)	107.1(6)	C(9)	–	C(10)	–	C(6)	108.3(7)
C(5)	–	C(1)	–	C(2)	108.0(6)	C(10)	–	C(6)	–	C(7)	108.3(6)
S(3)	–	C(21)	–	C(22)	122.5(6)	S(4)	–	C(11)	–	C(12)	118.8(5)
S(3)	–	C(21)	–	C(26)	115.5(6)	S(4)	–	C(11)	–	C(16)	121.9(5)
C(22)	–	C(21)	–	C(26)	121.9(7)	C(12)	–	C(11)	–	C(16)	119.2(6)
C(21)	–	C(22)	–	C(23)	118.3(8)	C(11)	–	C(12)	–	C(13)	120.3(6)
C(22)	–	C(23)	–	C(24)	120.8(9)	C(12)	–	C(13)	–	C(14)	120.3(7)
C(23)	–	C(24)	–	C(25)	120.2(8)	C(13)	–	C(14)	–	C(15)	119.7(6)
C(24)	–	C(25)	–	C(26)	121.2(8)	C(14)	–	C(15)	–	C(16)	120.7(7)
C(25)	–	C(26)	–	C(21)	117.7(8)	C(15)	–	C(16)	–	C(11)	119.8(6)

[a] Esds in parentheses refer to the last significant digit(s) of the preceding number.

[b] CNTR1 and CNTR2 are the centroids of the C_5H_5 rings, C1-C5 and C6-C10, respectively.

Table IV-8-6

Table 2. Atomic Parameters X,Y,Z and BISO for $Cp_2Ti(SC_6H_5)(SSSC_6H_5)$, E.S.DS. refer to the last digit printed.

|	X	Y	Z	BISO	
TI	0.56044(14)	0.42111(8)	0.34871(6)	3.02	(5)
S1	0.44595(23)	0.34128(13)	0.44508(10)	4.08	(9)
S2	0.5944 (3)	0.23356(14)	0.49413(11)	5.07	(10)
S3	0.5774 (3)	0.13062(14)	0.42060(12)	5.34	(10)
S4	0.52784(22)	0.30146(12)	0.25922(10)	3.69	(8)
C1	0.8405 (8)	0.4042 (6)	0.3196 (4)	4.9	(4)
C2	0.8229 (8)	0.4947 (5)	0.3403 (4)	5.0	(4)
C3	0.8133 (8)	0.4963 (5)	0.4151 (4)	4.7	(4)
C4	0.8245 (8)	0.4077 (5)	0.4406 (4)	4.2	(3)
C5	0.8387 (9)	0.3494 (5)	0.3816 (4)	4.3	(3)
C6	0.4579 (9)	0.5719 (5)	0.3555 (4)	4.6	(3)
C7	0.3422 (10)	0.5146 (5)	0.3810 (5)	5.7	(4)
C8	0.2617 (9)	0.4600 (5)	0.3210 (5)	5.8	(4)
C9	0.3304 (10)	0.4840 (5)	0.2594 (4)	5.3	(4)
C10	0.4515 (9)	0.5521 (4)	0.2807 (4)	4.4	(3)
C11	0.3091 (8)	0.2716 (4)	0.2211 (3)	3.1	(3)
C12	0.2509 (9)	0.2749 (4)	0.1442 (4)	3.9	(3)
C13	0.0835 (10)	0.2458 (5)	0.1120 (4)	5.1	(4)
C14	-0.0260 (9)	0.2130 (5)	0.1553 (4)	4.8	(4)
C15	0.0304 (9)	0.2101 (5)	0.2315 (4)	4.7	(4)
C16	0.1981 (8)	0.2389 (5)	0.2647 (4)	3.9	(3)
C21	0.3761 (9)	0.0761 (5)	0.4190 (4)	4.2	(3)
C22	0.2373 (10)	0.1191 (5)	0.4417 (4)	5.4	(4)
C23	0.0785 (11)	0.0731 (7)	0.4325 (5)	7.5	(5)
C24	0.0608 (13)	-0.0121 (7)	0.4036 (5)	8.7	(5)
C25	0.1976 (14)	-0.0530 (6)	0.3814 (5)	8.4	(6)
C26	0.3608 (12)	-0.0094 (5)	0.3895 (4)	6.2	(4)
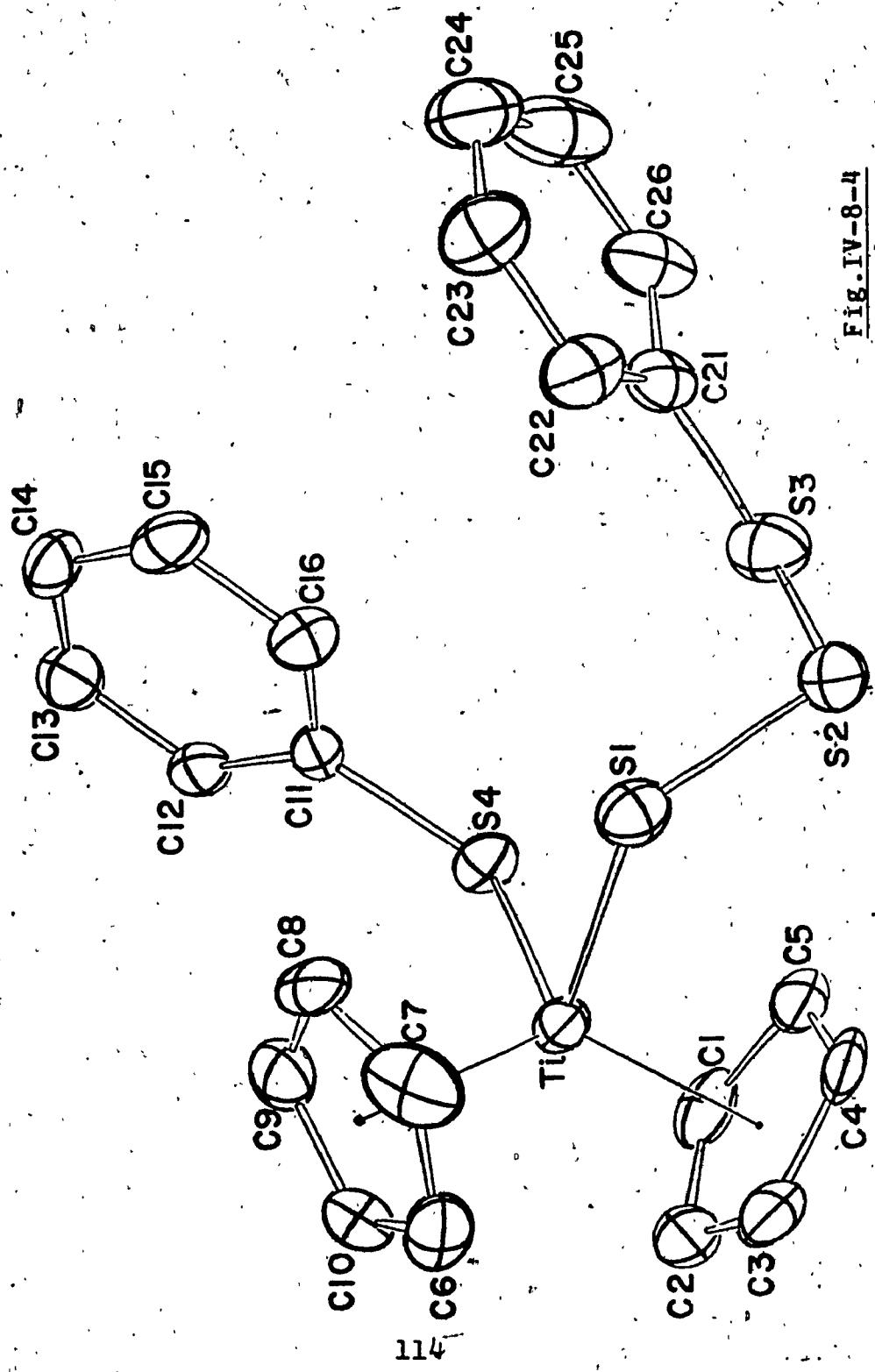
Fig. IV-8-4

114

IV-9 **CONCLUSION** :

The data obtained from the determination of the crystal structures of the three complexes as described in this thesis represent only an introductory survey. The main questions remain unanswered :

What facors influence the torsion angles in the $M-S_x-R$ chains and why are the two $M-S_2-R$ complexes so different in this respect?

Why does the stability of the chains vary. For example, why is the tungsten trisulphane unstable in the solid state and in solution, while the titanium trisulphane is stable in both? Why is the tungsten disulphane unstable in solution though stable in the solid state.

A much larger range of structures will need to be solved in order to detect trends which may have bearing on these questions.

REFERENCES

(1) E.S.Fedorov,Imperial St.Petersburg Mineralogical Soc.,23,99,(1887)

(2) E.S.Fedorov,Imperial St.Petersburg Mineralogical Soc.,24,345,(1890)

(3) A.Schoenflies,Krystallsysteme and Krystallstructur,-B.G.Teubner,Leipzig,(1891)

(4) E.S.Fedorow,Z.Krist.,21,679,(1893)

(5) W.Barlow,Z.Krist.,23,1,(1894)

(6) E.Von Fedorow,Z.Krist.,24,209,(1895)

(7) W.Barlow,Z.Krist.,25,86,(1896)

(8) E.Von Fedorow,Z.Krist.,25,113,(1896)

(9) W.Barlow,Mineral.Mag.,11,119,(1896)

(10) W.Barlow,Z.Krist.,29,433,(1896)

(11) W.L.Bragg,Proc.Cambridge Phil.Soc.,17,43,(1913)

(12) W.H.Bragg and W.L.Bragg Proc.Roy.Soc.,(London)(A),89,248,(1913)

(13) W.L.Bragg,Proc.Roy.Soc.,(London)(A),89,468,(1914)

(14) G.H.Stout and L.H.Jenson,"X-ray Structure Determination", McMillan,N.Y.,(1968)

(15) See ref.[14]

(16) D.E.Sands,"Introduction to Crystallography",Benjamin Inc.,(1969)

(17) L.V.Azaroff,"Elements od Crystallography",McGraw Hill,(1968)

(18) M.J.Burger,"X-ray Crystallography",Wiley,N.Y.,(1942)

(19) K.Weissenberg,Z.Physik.,23,229,(1942)

(20) E.W.Nuffield,"X-ray Diffraction Methods",Wiley,(1966)

(21) See ref.[14] and [18]

(22) M.J.Burger,"The Precession Method in X-ray Crystallography",Wiley,N.Y.,(1964)

(23) R.W.James,"The Optical Principles of the Diffraction of X-rays",Cornall Univ.Press,Ithaca,N.Y.,pp34-52,(1965)

(24) M.J.Burger,"Crystal Structure Analysis",Wiley,N.Y., pp29-48,(1960)

(25) E.Gabe,"The Data Collection Package",Crystallographic Division,National Research Council of Canada.

(26) NRC Program,"DATRD-2" Written at NRC by E.J.Gabe etal.

(27) M.J.Burger and G.E.Klein,J.Appl.Phys.,16,408,(1945)

(28) M.J.Burger and G.E.Klein,J.Appl.Phys.,17,285,(1946)

(29) G.H.Stout and L.H.Jensen,"X-ray Structure Determination,A Practical Guide",The McMillan,(1968)

(30) A.J.Wilson,Nature,150,152,(1942)

(31) H.Lipson and W.Cochran,"The Determination of Crystal Structures",G.Bell,London,pp38-46,(1957)

(32) ibid,pp12-15,(1957)

(33) ibid,pp76-109,(1957)

(34) G.H.Stout and L.H.Jenson,"X-ray Structure Determination" McMilan,N.Y.,pp267-269,(1968)

(35) A.L.Patterson,Phys.Rev.,46,372,(1934)

(36) A.L.Patterson,Z.Kryst.,A90,517,(1935)

(37) H.Lipson and W.Cochron,"The Determination of Crystal Structure",G.Bell,London,pp12-15,(1957)

(38) M.J.Burger,"Vector Space",Wiley,N.Y.pp41-64,(1954)

(39) M.F.C.Ladd and R.A.Palmer,"Theory and Practice of Direct Methods in Crystallography."Plenum Press,(1980)

(40) M.M.Woolfson,"Direct Methods in Crystallography",Oxford Univ.Press,(1961)

(41) G.N.Ramachandra and R.Srinivasan,"Fourier Methods in Crystallography",Wiley Interscience,(1970)

(42) J.Karle and I.L.Karle,Acta.Cryst.21,849,(1966)

(43) J.Karle,"Advances in Structure Research by Diffraction Methods",R. and B.Mason,Ed.,Wiley Interscience,N.Y.pp55-89,(1964)

(44) D.Sayer,Acta.Cryst.5,60,(1952)

(45) P.Main, M.Woolfson and G.Germain, Acta.Cryst., 1971.

(46) E.T.Whittaker and H.Robinson,"The Calculation of Observation",4thed.,Blackie and son.,Glasgow,pp209-259,(1944)

(47) E.W.Huges,J.Am.Chem.Soc.,63,1737,(1941)

(48) W.C.Hamilton,"Statistics in Physical Science",Ronald Press,N.Y.,pp124-577,(1964)

(49) W.E.Deming,"Statistical Adjustment of Data",Wiley,N.Y.,pp14-58,(1943)

(50) M.M.Woolfson,"X-ray Crystallography",Univ.Press.,(1970)

(51) NRC Program,"DIFFRAC" written at NRC by E.J.Gabe etal.

(52) NRC Program,"DATRD-2" written at NRC by E.J.Gabe etal.

(53) A.J.C.Wilson,Nature,150,152,(1942)

(54) NRC Program,"FOURR" written at NRC by E.J.Gabe etal.

(55) "MULTAN" written by P.Main;M.M.Woolfson and G.Germain.

(56) International Tables For X-ray Crystallography, Vol.IV, The Kynoch Press,Birmingham,England,(1974).

(57) NRC Program,"LSTSQ" written at NRC by E.J.Gabe etal.

(58) G.H.Stout and L.H.Jenson,"X-ray Structure Determination", McMilan,N.Y.(1968)

(59) NRC Program,"DISPOW" written at NRC by E.J.Gabe etal,

(60) NRC Program,"UNIMOL" written at NRC by E.J.Gabe etal.

(61) "ORTEP" written by Johnson.

(62) E.Block,"Reactions of Organosulphur Compounds"pp3 Academic Press,N.Y.(1978)

(63) B.M.Trost and L.S.Melvin,Jr.Sulphur Ylides.Academic Press,N.Y.(1975)

(64) S.Oae,"Organic Chemistry of Sulphur"pp45-67,328,Plenum Press,N.Y.(1977)

(65) Warren,B.E.;Burwell,J.T.;J.Chem.Phys.3,6,(1973)

(66) Schmidt,M.,Angew.Chem.Int.Ed.Engl.12,445,(1973)

(67) David,N.Harp,;Steliousk Chan,T.H.,J.A.C.S.100,1222,(1978)

(68) See ref [66]

(69) McCall,J.M.;Shaver,A.;J.Organomet.Chem.,193,C37-C39, (1980).

(70) Bird,P.H.;McCall,J.M.;Shaver,A.;Sriwardane,U.; Angew.Chem.Int.Ed.Engl.21,384-385,1982.

(71) See ref.69.

(72) H.D.Block and R.Allmann,Cryst.Struct.Comm.,4,53,(1975)

(73) B.R.Davis;I.Bernal and H.Kopf,Angew.Chem.Int.10.92,(1971)

(74) P.E.Jones and L.Katz,Chem.Comm.,842,(1976)

(75) J.Chatt and D.M.P.Mingos,J.Chem.Soc.(A),1243,(1976)

(76) E.G.Muller,;J.L.Patterson,;and L.F.Dahl,J.Organomet.Chem. 111,91,(1976)

(77) H.Waner, Z.Anorg.Allg.Chem.,30,464,(1980)

(78) See ref.76

(79) Harpp,D.N.;Ash,D.K.;Block,T.G.;Gleason,J.G.;Orwing,B.A.; Van Horn,W.F.;Snyder,J.P.,Tetrahedron Lett.pp3551-3554,(1970)

(80) Boustany,K.S.;Sullivan,A.B.,Tetrahedron.Lett.pp3547-3549,(1970)

(81) Harpp,D.N.; Ash,D.K. Internat.J.Of.Sulphur Chemistry. A,1,211-214, 1971.

(82) .

(83) Francesco,Caruso,;RiccardoSpagna,;and Luigi Zambovelli. Acta.Cryst.B36,pp713-715,(1980)

(84) Clive E.Briant,;Glyw R.Hughes,;Peter C.Minshall and D.Michael,;P.Mingos.J.Organomet.Chem.202,C21,(1980)

(85) Cattalini,L.;Michelon,G.;Marangoni,G.and Pelizzi,G.; J.Chem.Soc.Dalton.Trans.pp96-101,(1979)

(86) Carlos,A.L.Filgueiras,Philip,R.Holland,;Brian,F.G.Johnson

and Paul R.Raithby, Acta.Cryst.B38,pp954-956,(1982)

(87) Cattalini,L.Michelon,G;Marangoni G. and Pelizzi,G., J.Organomet.Chem.202,C21,(1980)

(88) Bird,P.H.;Lai,R.D.;Shaver,A.;Sriwardane,U.;Can.J.Chem. 60,pp2075-2081,(1982)

(89) See ref.[73]

(90) F.D.Rochou and R.Melanson,Acta.Cryst.B34,pp2138-2141,(1978)

(91) Zanotti,G.;DEL PraA.;Bombieri,G.and Tamburo A.M.,Acta.Cryst.B34,pp2138-2141,(1978)

(92) Rochou,F.D.;and Melanson,R.,Acta.Cryst.B36,pp691-693,(1980)

(93) Milburn,G.H.Trunter.J.C.S.(A),pp1609-1616,(1966)

(94) Melanson,R. and Rochon,F.D.,Acta.Cryst.B34,pp1125-1127,(1978)

(95) Sutton,L.E."Tables of Interatomic Distances and Configuration in Molecules and Ions",The Chemical Society,Burlington
House,London.Chem.Soc.Spec.Publ.No.11(1958) and 18(1965);Suppl. 1956-1959

(96) Laur,P.H."Sulphur in Organic and Inorganic Chemistry", Vol.2,Serring,A.Ed.M.Dekker,N.Y.(1972)

(97) The IUPAC Convention for linear polysulphur compound is that they be named Polysulohanes: Leoring,K.L.in "Sulphur in Organic and Inorganic Chemistry",Vol.3,(A)

121

Serring(ed),M.Dekker,Publ.N.Y. pp339-354,(1972).

(98) (a) Block,E.,J.Am.Chem.Soc.,95,pp5046-5048,(1973)

    (b) Bernard,D.J,Chem.Soc.,pp4675-4676,(1957)

    (c) Savige,W.E.;Fava A.,J.Chem.Soc.Chem.Comm.pp417-418
(1965)

(99) R.D.Adams,;D.M.Collins and F.A.Cotton,
Inorg.Chem.,13,pp1086,(1974)

(100) J.B.Wilford and H.W.Powell.J.Chem.Soc.(A),8,(1969)

(101) V.A.Semino and Yu.T.Struchkrov.,J.Struct.
Chem.9,pp931,(1968)

(102) M.Elder and D.Hall,Inorg.Chem.8,pp1273,(1969)

(103) E.M.Cradwick and D.Hall,J.Organomet.Chem.25,pp91,(1970)

(104) B.R.Davis and I.Bernal,J.Cryst.
Mole.Struct.2,pp195,(1972)

(105) R.Ros,;M.Vidali and R.Graziani,Gazzetta,100,407,(1970)

(106) M.G.B.Drew and A.P.Walters,J.C.S.Chem.Comm.pp457,(1972)

(107) R.M.Laine,;R.E.Moriarity and R,Bau.,J.Am.Chem.Soc.,94,
pp1402,(1972)

(108) (a) R.B.Peterson;J.J.Stezowski Che'ngwan;J.M.Burlitch
and R.E.Huges, J.Am.Chem.Soc.93,pp3532,(1971)

(109) Anthohy J.Conway;Graeme J.Ganisford;Roy R.Schrieke,
J.Chem.Soc.Dalton Trans.pp2499-2507,(1975)

(110) Scott.S.Woodard;Robert A.Jacobson;and Robert j.Angelici,
J.Organomet.Chem.117,C75-C80,(1976)

(111) Clifford Bueno and Melvyn Rowen Churchill,Inorg.Chem.,20

pp2197-2202,(1981)

(112) P.Michael Boorman;K.Amkerr;and Vikram D.Patel.J.C.S. Dalton Trans.,pp506-510,(1981)

(113) D.Coucouvanis;P.Stremple;E.D.Simhon;,Inorg.Chem.,22, pp293-308,(1983),and refrences there in.

(114) Michael G.B.Drew;Gerald W.A.Fowles;Elizabeth M.Page and David A.Rice,J.C.S.Dalton Trans.pp2409-2413,(1981)

(115) See ref.[82] and [83]

(116) Kubacek,P.;Hoffman,R.;Havlas,Z.,J.Organomet. Chem.,1,pp180-188,(1982)

(117) J.A.C.S.,103,pp159-168,(1981) and references there in.

(118) Shaver,A.;Hartgerink,J.;Lai,R.D.;Bird,P.;Ansari,N.,J.Organomet.Chem. 7,938-940, (1983)

(119) Only one slightly broadened resonance was observed for the methyl groups in 2 in its ^{1}H nmr spectrum. The chemical shift of the methyl group in p-tolyl polysulphanes is not sensitive to chain length.

(120) Muller,E.G.; Watkins,S.F.; Dahl,L.F.; J.Organomet.Chem.111, 73-89, 1976.

(121) Laur,P.H. in "Sulphur in Organic and Inorganic Chemistry". Vol.3, Senning,A.Ed.,M.Dekker,N.Y.1972.

(122) See ref.[121].

(123) See ref.[73 and 77]

(124) T.C.McKenzie,R.D.Sanner and J.E.Bercaw, J.Organomet.Chem.102,457,1975.